## ABSTRACT

MOORE, ANDREW MACKIN. The Effect of Biomass Characteristics on Bio-oil Produced via Fast Pyrolysis. (Under the direction of Dr. Sunkyu Park and Dr. Richard Venditti).

Renewable energy has become an increasingly important topic since the turn of the century. With variable oil prices, regulations on emissions, and global warming, a push is needed to develop domestic sources of renewable energy. Of particular concern are renewable transportation fuels as these power our vehicles and thus our economy. The US in general has enormous and vast forests, particularly in the southeast, that can be harvested and converted into useable, renewable fuels. Thermochemical conversion of biomass is a promising way of producing these fuels, and fast pyrolysis is at the forefront. Much research has been put into advancing the knowledge of fast pyrolysis to make it a feasible technology to produce useable bio-oil, but there is still much to learn. Due to its high temperatures, reactions occur rapidly and are extremely numerous. The variability of the feedstocks compounds the complexity of fully understanding the reactions, mechanisms, and processes of the fast pyrolysis of lignocellulosic biomass.

In order to advance the understanding of the effect the biomass composition has on the fast pyrolysis process; several studies were developed and executed. The cellulose portion of lignocellulosic biomass is the most abundant and thus it is expected to be of the most important to study. Cellulose has two primary properties which are the crystallinity and degree of polymerization (DP). The first study successfully separated the two properties and analyzed them individually. The results showed the levoglucosan, a primary product of cellulose pyrolysis, increased as both DP and the crystallinity index decreased. Along with that, the lower DP samples produced levoglucosan earlier in pyrolysis.

In order to progress towards using whole lignocellulosic biomass samples, other studies were planned, again to understand some effect of feedstock properties on bio-oil. The addition of calcium formate to the feedstock was proposed in order to decompose and produce reactive hydrogen to reduce to total oxygen content of the final bio-oil. Several preparation methods were used, and these had a profound impact on the water content of the bio-oils produced. Samples prepared via an acid-base reaction had almost twice the water content in the condenser bio-oil as the raw biomass. Calcium formate was shown to decompose in the regime of cellulose via TGA, confirming the production of $H_2$. Overall, a high calcium formate amount did not lead to a significant decrease in the final oxygen content of the bio-oil, nor the O/C ratio. Slightly reduced oxygen contents were seen for a few samples, but they were accompanied by a decrease in yield. Ultimately the calcium formate did not impact the pyrolysis significantly, whereas the preparation method did.

The final study investigated the effect of increasing lignin content on the fast pyrolysis process. Waste lignin, Acetosolv, was added to biomass systematically to measure its effect on the bio-oil, while also demonstrating that process lignin can be utilized for production of bio-oil. Total oil yields decreased as expected when additional lignin was added. As the lignin addition increased, char, pyrolytic water yields and acids content increased due to the presence of aliphatic and oxygenated side-chains within the isolated lignin's structure. TGA and SEM were used to explain some unexpected results, and it was discovered that a thin non-permeable layer could exist, hindering the production of volatiles, specifically for a moderate lignin increase.

© Copyright 2015 Andrew Mackin Moore

All Rights Reserved

# The Effect of Biomass Characteristics on Bio-oil Produced via Fast Pyrolysis

by
Andrew Mackin Moore

A thesis submitted to the Graduate Faculty of
North Carolina State University
in partial fulfillment of the
requirements for the degree of
Master of Science

Forest Biomaterials

Raleigh, North Carolina

2015

APPROVED BY:

| | |
|---|---|
| _____ | _____ |
| Dr. Sunkyu Park<br>Committee Co-Chair | Dr. Richard Venditti<br>Committee Co-Chair |
| _____ | _____ |
| Dr. David C. Tilotta | Dr. Elon Ison |

## DEDICATION

I wish to dedicate this thesis to my loving girlfriend Ema Ciglič. She has been with me through my graduate school and I don't know where I would be without her. She makes me smile more than anyone else and has always been there when I needed. Even from thousands of miles away she makes me feel like the most special guy on earth.

## BIOGRAPHY

Andrew Mackin Moore, who goes by Drew, was born on August 24, 1988 in Charlotte, NC to Kim and Ellen Moore. He grew up with his three brothers Ryan, Jordan, and Greg. Drew graduated from Ashbrook High School in June 2006 summa cum laude. He began his undergraduate studies at North Carolina State University in the fall of 2006. He received a Pulp and Paper Foundation scholarship to dual major in Paper Science and Engineering as well as Chemical Engineering. During his undergraduate career, Drew successfully completed two summer internships; one at Kapstone Paper and Packaging in Roanoke Rapids, NC in 2008, and another at Cascades Tissue Group in Rockingham, NC in 2010. Drew graduated in December 2010 magna cum laude.

Drew began his graduate career at NC State in January 2011 in the department of Forest Biomaterials under the direction of Dr. Sunkyu Park and Dr. Richard Venditti on an NNF fellowship. His research topic was related to the thermochemical conversion of biomass to biofuels. From June to December 2014, he had the opportunity to travel to Chile and continue his research at UDT as a part of the University of Concepcion under the direction of Dr. Marion Carrier.

## ACKNOWLEDGMENTS

I want to thank Dr. Park and Dr. Venditti for their research advice, guidance, and support. I also want to thank Dr. Tilotta for his never-ending GC-MS support and for serving on my committee. Thank you to Dr. Ison for serving on my committee and being the Chemistry department representative and allowing me to pursue my minor. These four people have assisted and helped me along the way and allowed me to finish my studies.

I would also like to express my gratitude to Dr. Hasan Jameel and Dr. Hou-min Chang for their organization of the bioenergy group and research advice, Dr. Kelley for his support and knowledge, all other Forest Biomaterials professors for teaching me, Brandon Jones, who went through this entire ordeal with me, Dr. Jiajia (August) Meng who was my mentor and helped me out so much in my first years, Dr. Jun Park, Lu Liu, Ren Xueyong, Melissa Rabil, Barbara White, and Mike Maltby all for their help.

I also want to give thanks to my parents, brothers, family, and friends for supporting me during my studies and for being there when I needed it most. You guys are the best and mean everything to me. Another big thanks goes to Ema for talking with me day in and day out and taking all the frustration from me. Finally, thank you to my God, for allowing all of this and everything to be possible.

## TABLE OF CONTENTS

## LIST OF TABLES

## LIST OF FIGURES

# CHAPTER 1

## Effect of Crystallinity and Degree of Polymerization on the Fast Pyrolysis Decomposition Products of Cellulose

### 1. Introduction

Interest in bio-fuels produced from renewable resources has grown tremendously in recent years due to increasing petroleum prices from dwindling supplies, growing environmental concerns about greenhouse gases, and government policies. The US has an abundance of natural forests which have the potential to be converted into a clean, cheap, and efficient source of fuel. Woody biomass is composed primarily of cellulose, about 40% dry weight basis, and the most abundant natural compound on Earth (Sjöström). Cellulose is composed of linearly linked β–D-glucopyranose units. A single cellulose chain can be up to 15,000 units long based on its source and how it was processed (Cheng). Cellulose has been used extensively to produce ethanol through biochemical pathways, the most popular thermochemical conversion technique has seen much less focus. Fast pyrolysis uses very fast heating rates to produce a liquid product which can be further upgraded to produce an oil similar to that of petroleum oil (Bridgwater, Meier and Radlein). Due to the nature of the reactions and environment, the mechanism for the thermal breakdown of cellulose is not fully understood. The primary product from the pyrolysis of cellulose is levoglucosan, with yields of up to 58% for pure cellulose samples. Levoglucosan can be easily hydrolyzed into glucose for ethanol production or converted directly into ethanol via levoglucosan kinase containing organisms (Jarboe et al.).

Cellulose pyrolysis has been studied as early as 1918 by Pictet and Sarasin (Pictet and Sarasin). Fast pyrolysis is a simple technology, but deals with complex reactions involving three phases and many competing reactions. Due to the speed of the reactions and high temperatures that they take place in, it is difficult to determine the exact mechanisms of cellulose pyrolysis. In the 1970's Shafizadeh began working on using cellulose pyrolysis as a potential renewable fuel source through the production of levoglucosan (Shafizadeh and Bradbury; Shafizadeh and Fu). Several groups have attempted to determine the mechanism of levoglucosan formation from cellulose. Mayes et al. covered a number of the proposed mechanisms for the formation of levoglucosan (Mayes and Broadbelt). Previous attempts to discern how cellulose is degraded have lumped products into groups such as volatiles, char, gas, etc (Broido and Nelson; Bradbury, Sakai and Shafizadeh; Ranzi et al.). More recent attempts using modeling have elucidated and identified the most probable pathways for compounds to be formed from a model cellulose compound, methyl cellobiose (Mayes and Broadbelt). The focus compound for cellulose pyrolysis is levoglucosan, which is the most abundant product from cellulose and glucose. There has been considerable controversy over the mechanism of levoglucosan from cellulose, specifically for the initial breaking of glycosidic bond occurs via heterolytic or hemolytic bond cleavage (Mohan, Pittman and Steele; Shen and Gu; Ponder, Richards and Stevenson). Broadbelt determined that a one-step concerted reaction had a much lower energy barrier and a faster rate coefficient by several orders of magnitude (Mayes and Broadbelt).

While there is ongoing research in using cellulose model compounds and computer simulations to understand how cellulose thermally degrades, there is not as much focus on

experimental data to back up the simulations. Additionally, the physical characteristics of the cellulose could play an important role in how the cellulose is decomposed. Much of the research looking at physical characteristics revolves around TGA, which is not fully indicative of the fast pyrolysis process. The primary physical characteristics of cellulose are crystallinity and chain-length. Another major issue with past research attempts are the failure to isolate the effects of either property. Ball-milling is often used as an easy method to reduce the crystallinity of cellulose, however, the physical forces will also severely degrade the cellulose, thus affecting the DP as well. Therefore, the purpose of this research is to isolate the effects of the chain-length and crystallinity on the fast pyrolysis products from cellulose.

The effects of crystallinity have been investigated in the past, albeit not thoroughly. Wang et al. found that amorphous samples degraded through a liquid intermediate, while the more crystalline samples did not show an indication of this phenomenon (Wang et al.). With respect to product distribution, higher yields of levoglucosan were reported for the more crystalline samples, while the lower crystallinity samples showed higher yields of furanic compounds. Other results suggest that crystalline cellulose produces higher amounts of levoglucosan and amorphous cellulose leads more to char and gas formation.

The cellulose chain length can vary significantly between all biomass as well as cellulose produced by different methods. The lowest DP for cellulose is 2, cellobiose, whereas some other forms of cellulose can reach 15,000 units long (Cheng). The chain length of cellulose has been investigated in the past. The chain length is very challenging for computer simulations to handle, as the CPU time needed for the analysis increases exponentially (Mettler, Vlachos and Dauenhauer). Researchers have looked to use a modified

fast pyrolysis process, thin-film pyrolysis, to look at the effect of DP on low DP cellulose samples. They determined that some compounds, such as levoglucosan, increase as DP increases (Mettler et al.).

The specific objective of this study are to produce a unique set of cellulose samples which will lead to the separation of the effects of cellulose crystallinity and degree of polymerization on the products generated via fast pyrolysis. By separating these two important properties, we hope to gain knowledge into cellulose pyrolysis.

## 2. Materials and Methods

### 2.1 Cellulose Samples

Whatman filter paper 1 was used as the starting cellulose material for this study. Amorphous cellulose was prepared by dissolution in DMSO as methylol cellulose as described by Schroeder et al. (Schroeder, Gentile and Atalla). Amorphous cellulose was precipitated in a stirred bath of sodium methoxide in methanol and propanol before washing and freeze-drying. The samples with reduced degree of polymerization (DP) were produced using a modified filter paper unit procedure. Briefly, 0.25g cellulose samples were mixed with 15mL of buffer and enzyme (NS 50013, Novozymes Inc.) at varying concentration. The samples were incubated in a shaking water bath for one or two hours and washed extensively before freeze-drying (Yu et al.).

## 2.2 Bicinchoninic acid assay (BCA)

DP of cellulose samples were calculated by reducing end analysis (Kongruang et al.). A 1mL aliquot of cellulose suspension was added to 1mL of BCA working reagent. The samples were incubated at 80°C for 30 min. before centrifugation and separation. The absorbance, at 560 nm, of the supernatant was measured by a Perkin-Elmer UV-Vis detector. A calibration curve was generated from 0-50μM glucose to determine the nanomoles of reducing ends per milligram of cellulose. The average DP (glucose monomers) of the cellulose sample was then calculated from the number of reducing groups.

## 2.3 X-Ray Diffraction (XRD)

XRD was performed on a Rigaku SmartLab x-ray diffractometer with Cu radiation source. Samples were scanned from 2θ of 9 to 41 with a step change of 0.05. CrI was calculated based on an amorphous subtraction method used by Park et al. (Park et al.).

## 2.4 Fiber Quality Analysis (FQA)

A Perkin-Elmer Fiber Quality Analyzer was used to measure the average fiber width for each cellulose sample. A fiber count of 5000 was employed and the method of analysis was ISO 2009.

## 2.5 Thermogravimetric analysis (TGA)

TGA was performed on a TA Instruments Q500 thermogravimetric analyzer. The temperatures ranged from 25-900°C with a heating rate of 10°C/min. The analysis was

performed in nitrogen and then switched to air after 15 min at 900°C to determine the ash content, as per the ASTM E1131-08 method. The TGA and DTG curves were measured for onset points and maximum weight loss temperature in addition to the proximate analysis.

2.6 Pyroprobe-Gas Chromatography/Mass Spectrometry (Py-GC/MS)

Py-GC/MS analysis was performed on a CDS analytical model 5150 pyroprobe connected to a GC/MS system. 500±30μg of cellulose was placed in a quartz tube with 3±0.1mg of quartz wool. Gas chromatography/mass spectrometry analyses of the pyrolysis vapors were performed on a Finnigan Polaris Q Plus system. The MS detector was set at a full scan mode with a mass to charge range from 10 to 450 amu. Standard electron impact (EI) ionization at 70 eV was employed and the ion source temperature was 200 °C. The GC column used for separation was a DB-1701 column 60 m × 0.25 mm with 0.25 μm film thickness. The GC oven temperature was initially held at 45 °C for 4 min, then ramped at 3 °C/min to 280 °C, and held at 280 °C for 15 min. The injector and detector temperatures were set at 250 and 280 °C, respectively. The injector split ratio was fixed at 100:1. The pyroprobe was set to 600°C to reach a sample temperature of 500°C, and then held for 15 seconds (Ronsse et al.). The heating rate was set to infinite to reach the set-point almost immediately. The interface temperature was set to 280°C and transfer line temperature was 250°C to minimize condensation of vapors prior to the GC. High purity helium was employed as the GC carrier gas at a flow rate of 38 cm/min, and duplicate tests were performed for each analysis. Compounds were identified based on comparative analysis of references and the NIST library.

## 2.7 Molecular beam mass spectrometry

MBMS was performed at the National Renewable Energy Laboratory (NREL). About 10 mg of samples were heated to 500°C in a boat and swept into the sample chamber by helium gas. The volatile products were hit with an ionization energy of 22.5 eV. The scan range was from 30-150 amu and the raw data was compiled with The Unscrambler® multivariate analysis software.

# 3. Results and Discussion

## 3.1 Cellulose characterization

Two sets of cellulose samples were prepared as described before and the results of the physical characterization are shown in Table 1.1. The samples labeled CrI are the samples used in the crystallinity study, and the samples labeled DP are included in the DP study. The DP of the samples in the crystallinity study are all approximately 4000 and have crystallinities varying from 0 to 79.4. In the DP study, the crystallinity of the samples remain at ~83, while the DP ranges from 457 to 3535. Table 1.2 shows the proximate analysis of the cellulose samples determined by TGA. In all samples, ash content was consistent and less than 0.5% and is considered a non-factor for this study. Likewise, the limiting factor for heat transfer in the fiber is the expected to be the fiber width, which is verified to be quite similar in all samples. The specific TGA curves are shown in Figure 1.1. The heating rate, 100°C/min, was maximized for the proximate analysis to reach as close to fast pyrolysis as possible. There appeared to be no change in the degradation onset between the samples. The

volatiles amount varied slightly between the samples, but none varied significantly. Under the slow pyrolysis conditions, the cellulose samples behave similarly, and neither the DP nor the crystallinity have any noticeable effects.

### 3.2 Effect of DP on pyrolysis products

The yield of each component was calculated by dividing the peak area of the specific compound by the total peak area of the spectra and they are plotted in Figure 1.2. The amount of cellulose added to each sample was held as close to 0.50mg as possible, but the amount pyrolyzed varied slightly, ±0.05mg. However, regardless of the amount pyrolyzed or the total peak area measured, a comparison between components as a fraction of the whole can be made. The results can be seen as semi-quantitative and thus can be compared between the different cellulose samples. Figure 1.2a shows the effect of DP on levoglucosan yield for five cellulose samples. From a chain length of about 450 to 1350, there is an almost linear decrease in the levoglucosan yield as the DP increases. After this point, the DP does not appear to affect the yield of levoglucosan. In the regime between 450-1350, the levoglucosan yield drops over 30%. Studies on active cellulose have shown that during this proposed initiation step, the DP decreases to near 200 (Broido et al.; Shafizadeh and Bradbury). The reducing ends have been shown to be important reactive sites for the thermal decomposition of cellulose (Matsuoka, Kawamoto and Saka "Reducing End-Group of Cellulose as a Reactive Site for Thermal Discoloration"; Matsuoka, Kawamoto and Saka "Thermal Glycosylation and Degradation Reactions Occurring at the Reducing Ends of Cellulose During Low-Temperature Pyrolysis"). Mamleev et al also showed that the reducing ends of

cellulose are necessary for the pyrolysis of cellulose and once formed, the cellulose chain proceeds to degrade by “unzipping” (Mamleev, Bourbigot and Yvon). As the samples with lower DP have more thermally reactive reducing ends, it can be reasonably expected that they can more easily degrade into the primary product of levoglucosan. It is unclear whether or not cellulose transitions to active cellulose under fast pyrolysis conditions (heating rates >1,000°C/s), but evidence shows it is likely to occur under slow pyrolysis conditions (Matsuoka, Kawamoto and Saka "What Is Active Cellulose in Pyrolysis? An Approach Based on Reactivity of Cellulose Reducing End"). Other research has shown an increase in LG production as DP increases (Mettler et al.). They saw an increase in LG between chain length of 1 and 133. This could indicate another regime of DP<500 where LG yield increases as DP increases, with a possible maximum at 200 for active cellulose. The increase in LG yield at low DP, could be explained by an increase in mobility of the cellulose chains. Fast pyrolysis of cellulose has been shown to undergo a liquid intermediate before ejecting aerosols (Shafizadeh and Bradbury). With shorter cellulose chains, there may be more mobility in the cellulose structure, allowing this molten cellulose state to be achieved more quickly. It has been reported that one of the first steps in cellulose pyrolysis is the breakdown into small chain anhydro-oligomers (Y. C. Lin et al.). Pyrolysis of cellulose samples with an already decreased chain length can thus reach these anhydro-oligomers more rapidly and easily than a larger chain. Additionally, a conformation change from a chair to a boat conformation allows for the C6 hydroxyl oxygen to attack the anomeric carbon. With the improved mobility of a shorter cellulose chain, the conformation change can be more easily achieved, thus initiating the degradation of cellulose into levoglucosan.

It is believed that the effective cleavage of the β-1,4-glycosidic linkage is the key step that determines the rate of LG formation from fast pyrolysis, regardless of the type of reaction mechanism hypothesized. The number of chain ends also determines the rate of LG formation because LG is released from them, and once this process starts, it is more likely to proceed sequentially along the chain. As shown in Figure 1.3, two cellulose chains ("b" and "c") can be formed from the native cellulose ("a"). By beginning with these shorter cellulose chains, the chances of producing LG from cellulose are enhanced in the subsequent pyrolysis process as these cellulose chains undergo the same pyrolysis reaction to its parent chain. More importantly, the new cellulose chain possesses a 1,6-anhydro-linkage at the reducing end ("b" and "d"), in which a molecule of LG can be quickly released for each subsequent scission of the glycosidic bond.

Table 1.3 shows the yields for all identified products from the Py-GC-MS. The changes for these minor products were far less pronounced than for LG. The furanose form of LGA (LFA) expectedly mirrored the trend set in fig. 1. While glycolaldehyde and acetol can degradation products of levoglucosan, they can also be formed via ring opening of glucose, shown as pathway 2 in Figure 1.3. Under the rapid conditions of fast pyrolysis, it is reasonable that the levoglucosan is quickly removed and does not undergo secondary decomposition. Glycolaldehyde and acetol content increase as DP increases, further supporting the idea that under these conditions they are competing reactions with LGA. Other products, such as furans (hydroxylmethylfurfural and furfural do not appear to be affected by the chain length.

3.3 Effect of crystallinity on pyrolysis products

Figure 1.4a shows the effect of crystallinity on LG production. Three samples were included based on constant DP values and varying crystallinity index values (FP-EH-18, FP-CrI-01, and FP-CrI-03). The highest value for LG yield was from FP-CrI-03 at 49.87%, while the lowest value was 35.35% for FP-EH-18. This indicates that there is a substantial influence of crystallinity on the amount of levoglucosan produced. Previous studies have shown that more crystalline cellulose leads to a higher levoglucosan production. Our results contradict that and show that at the same DP, a more amorphous cellulose will produce more than a more crystalline one. The crystallinity is an indirect measure of the amount of hydrogen bonding between the cellulose fibers. The hypothesis is that a more amorphous sample would produce more LGA than a more crystalline sample due to the additional energy needed to break the hydrogen bonds in the crystalline sample. Additionally, it has been mentioned previously that a liquid intermediate occurs for fast pyrolysis of cellulose. With the lack of a crystal structure, the low crystallinity samples will proceed to melt and release levoglucosan in a higher abundance.

In addition to a higher yield of LGA from the amorphous sample, more gas, GA, and HMF are formed, but with much lower amounts, Figure 1.4b. In fact, the amorphous sample produces slightly more of nearly every compound studied, Table 1.3. The reasoning behind this is somewhat unknown, but may be related to a better pyrolysis efficiency for the lower crystallinity samples as they would be easier to pyrolyze with fewer hydrogen bonds to break before forming volatile compounds from the cellulose intermediate. As expected, LFA mirrors the LGA trend with more produced at lower crystallinity. With regards to the furanic

compounds studied, more are produced at low crystallinity. As previously reported, furanic compounds are favored at lower crystallinity due to enhanced dehydration reactions.

Crystallinity is a measure of the amount of hydrogen bonding in cellulose, and thus, by reducing the crystallinity, the amount of hydrogen bonding will be reduced. In addition, the presence of a short-lived liquid phase during the pyrolysis of cellulose was observed as amorphous cellulose and a change from its chair to boat formation might be necessary for forming LG. Therefore, breaking hydrogen bonds and increasing the amorphous proportion of cellulose by heat treatment would facilitate the conformational change of the cellulose macromolecules required to form LG.

### 3.4 MBMS analysis

Molecular beam mass spectrometry was utilized to determine the products produced from cellulose samples immediately after being produced. MBMS has the advantage that no secondary or decomposition products can be formed and all mass spectra are measured at once, so it can provide product information as a function of time. The raw data was first extracted and then principal component analysis was performed. Based on this analysis, three principal components were determined (PC-1, PC-2, and PC-3) and the mass spectra for these components are shown in Figure 1.5. Based on these mass spectra and comparing to known compounds produced from cellulose pyrolysis, the primary species dominating each spectra can be revealed. With large peaks at m/z of 57, 60, and 73, PC-1 can be easily identified as primarily levoglucosan. Key m/z values for PC-2 include 31, 42, 69, 97, and 128 which point towards PC-2 being mostly glycolaldehyde and 5-HMF. PC-3 had m/z peaks at

31, 43, 57, 60, 73, 97, and 126. This range of values points towards PC-3 being a combination of secondary products from LG. Each component accounted for a specified variance between the samples, 95% for PC-1, 4% for PC-2, and 1% for PC-3.

Figure 1.6 shows the three components yield at given time points during pyrolysis of FP-control. Initially, large amounts of component 1 (LG) are rapidly produced. After reaching a peak yield of ~6.5%, less and less is produced as more of the cellulose is being consumed. The yield then decreases linearly until the experiment is done. Component 2 follows a similar trend to component 1 indicating that it is not a product of component 1.

Due to the unique time sensitive measurements of MBMS, additional information can be gathered about the effects of DP and CrI. Figure 1.7 shows that lower DP samples tend to produce LG earlier in the pyrolysis process than higher DP samples. The samples with DP of 431 and 1231 are the first to produce LG at times of 4 and 3 seconds respectively. While the sample with the highest DP, 2918 and 1838, are the last to show levoglucosan production, at 7 seconds for the former and 6 seconds for the latter. This observation supports the theory that chain length needs to be shortened as a first step in the pyrolysis pathways.

## 4. Conclusions

Py-GC/MS and Py-MBMS were employed on cellulose samples with varying levels of crystallinity and DP, with the intent of isolating the effects of both of these parameters. Careful preparation techniques were used to generate two sets of samples, one with a constant DP and varying levels of CrI, and another with a constant CrI and varying levels of DP, all from the same starting material. By eliminating as much sample variation as possible,

it is possible to gather information that may have been convoluted by overlap and various interactions.

Both the crystallinity and DP were shown to have effects on the product distributions. There was no change in the types of products produced, but the amounts varied substantially. The primary compound of interest was levoglucosan, LGA, as it is the largest product of cellulose pyrolysis, accounting for up to 60% of the product distribution. LGA was shown to be produced in much higher quantities at the lowest DP value measured and then leveled off after around 1300. The higher amount of LGA produced at lower DP is attributed to the decomposition pathway of cellulose going through small chain anhydro-oligomers. With a lower DP, these are formed more readily and can then decompose further into LGA. Several other compounds were also dependent on DP, including glycolaldehyde and permanent gases. These showed the opposite trend of LGA, indicating either a competing reaction or a secondary reaction or a combination of both.

The crystallinity did not have as significant an effect as the DP on LGA production. Again though, a lower crystallinity favored LGA production, but unlike the DP, there was no leveling off. In agreement with other researchers, our results showed that furanic compounds were preferentially produced at lower crystallinities due to enhanced dehydration reactions.

A key point was that the ash content of each sample are similar, ruling out any effects of inorganics on the results.

Based on these results, it would appear the ideal biomass for producing LGA, would be one with a very low DP and a very low CrI. However, this may not be the case, as this would mean a ball-milled sample should produce the highest amount of LGA. In fact, cotton

fibers have a very high yield of levoglucosan. This means there may actually be some crystal structure or chain-length needed for optimum LGA production.

## 5. Acknowledgements

This study was supported by the United States Department of Agriculture National Needs Fellowship program (USDA NNF)

## REFERENCES


Bradbury, Allan GW, Yoshio Sakai, and Fred Shafizadeh. "A Kinetic Model for Pyrolysis of Cellulose." Journal of Applied Polymer Science 23.11 (1979): 3271-80. Print.

Bridgwater, AV, D Meier, and D Radlein. "An Overview of Fast Pyrolysis of Biomass." Organic Geochemistry 30.12 (1999): 1479-93. Print.

Broido, A, et al. "Molecular Weight Decrease in the Early Pyrolysis of Crystalline and Amorphous Cellulose." Journal of Applied Polymer Science 17.12 (1973): 3627-35. Print.

Broido, A, and Maxine A Nelson. "Char Yield on Pyrolysis of Cellulose." Combustion and Flame 24 (1975): 263-68. Print.

Cheng, Jay. Biomass to Renewable Energy Processes. CRC Press Inc., 2010. Print.

Jarboe, L. R., et al. "Hybrid Thermochemical Processing: Fermentation of Pyrolysis-Derived Bio-Oil." Appl Microbiol Biotechnol 91.6 (2011): 1519-23. Print.

Kongruang, S., et al. "Quantitative Analysis of Cellulose-Reducing Ends." Applied Biochemistry and Biotechnology 113 (2004): 213-31. Print.

Lin, Y. C., et al. "Kinetics and Mechanism of Cellulose Pyrolysis." Journal of Physical Chemistry C 113.46 (2009): 20097-107. Print.

Mamleev, V., S. Bourbigot, and J. Yvon. "Kinetic Analysis of the Thermal Decomposition of Cellulose: The Main Step of Mass Loss." Journal of Analytical and Applied Pyrolysis 80.1 (2007): 151-65. Print.

Matsuoka, S., H. Kawamoto, and S. Saka. "Reducing End-Group of Cellulose as a Reactive Site for Thermal Discoloration." Polymer Degradation and Stability 96.7 (2011): 1242-47. Print.

---. "Thermal Glycosylation and Degradation Reactions Occurring at the Reducing Ends of Cellulose During Low-Temperature Pyrolysis." Carbohydrate Research 346.2 (2011): 272-79. Print.

---. "What Is Active Cellulose in Pyrolysis? An Approach Based on Reactivity of Cellulose Reducing End." Journal of Analytical and Applied Pyrolysis 106 (2014): 138-46. Print.

Mayes, H. B., and L. J. Broadbelt. "Unraveling the Reactions That Unravel Cellulose." J Phys Chem A 116.26 (2012): 7098-106. Print.

Meng, Jiajia. *Converting Biomass into Renewable Fuel Intermediate-Bio-Oil: Elucidating Torrefaction Effect on Bio-Oil Quality and Study on Bio-Oil Aging Mechanism*. North Carolina State University, 2013. Print.

Mettler, Matthew S., et al. "The Chain Length Effect in Pyrolysis: Bridging the Gap between Glucose and Cellulose." Green Chemistry 14.5 (2012): 1284. Print.

Mettler, Matthew S., Dionisios G. Vlachos, and Paul J. Dauenhauer. "Top Ten Fundamental Challenges of Biomass Pyrolysis for Biofuels." Energy & Environmental Science 5.7 (2012): 7797. Print.

Mohan, D., C. U. Pittman, and P. H. Steele. "Pyrolysis of Wood/Biomass for Bio-Oil: A Critical Review." Energy & Fuels 20.3 (2006): 848-89. Print.

Park, S., et al. "Cellulose Crystallinity Index: Measurement Techniques and Their Impact on Interpreting Cellulase Performance." Biotechnol Biofuels 3 (2010): 10. Print.

Pictet, Amé, and Jean Sarasin. "Sur La Distillation De La Cellulose Et De L'amidon Sous Pression Reduite." Helvetica Chimica Acta 1.1 (1918): 87-96. Print.

Ponder, Glenn R, Geoffrey N Richards, and Thomas T Stevenson. "Influence of Linkage Position and Orientation in Pyrolysis of Polysaccharides: A Study of Several Glucans." Journal of analytical and applied pyrolysis 22.3 (1992): 217-29. Print.

Ranzi, Eliseo, et al. "Chemical Kinetics of Biomass Pyrolysis." Energy & Fuels 22.6 (2008): 4292-300. Print.

Ronsse, Frederik, et al. "Optimization of Platinum Filament Micropyrolyzer for Studying Primary Decomposition in Cellulose Pyrolysis." Journal of Analytical and Applied Pyrolysis 95 (2012): 247-56. Print.

Schroeder, Leland R., Victor M. Gentile, and Rajai H. Atalla. "Nondegradative Preparation of Amorphous Cellulose." Journal of Wood Chemistry and Technology 6.1 (1986): 1-14. Print.

Shafizadeh, F., and A. G. W. Bradbury. "Thermal-Degradation of Cellulose in Air and Nitrogen at Low-Temperatures." Journal of Applied Polymer Science 23.5 (1979): 1431-42. Print.

Shafizadeh, Fred, and YL Fu. "Pyrolysis of Cellulose." Carbohydrate Research 29.1 (1973): 113-22. Print.

Shen, D. K., and S. Gu. "The Mechanism for Thermal Decomposition of Cellulose and Its Main Products." Bioresour Technol 100.24 (2009): 6496-504. Print.

Sjöström, Eero. Wood Chemistry: Fundamentals and Applications. Access Online via Elsevier, 1993. Print.

Wang, Zhouhong, et al. "Effect of Cellulose Crystallinity on the Formation of a Liquid Intermediate and on Product Distribution During Pyrolysis." Journal of Analytical and Applied Pyrolysis 100 (2013): 56-66. Print.

Yu, Z., et al. "Evaluation of the Factors Affecting Avicel Reactivity Using Multi-Stage Enzymatic Hydrolysis." Biotechnol Bioeng 109.5 (2012): 1131-9. Print.

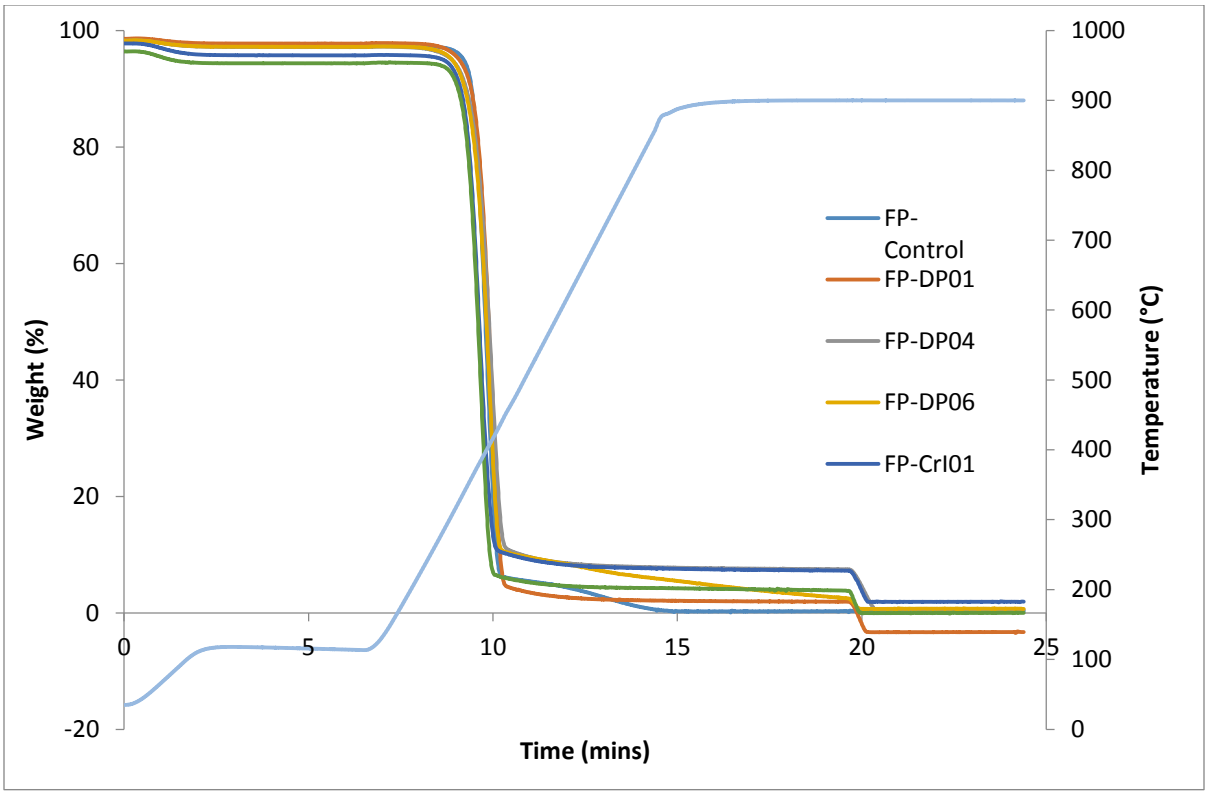


**Figure 1.1** TGA of select cellulose samples. Heating ramps: 50°C/min to 110°C, 100°C/min to 900°C.

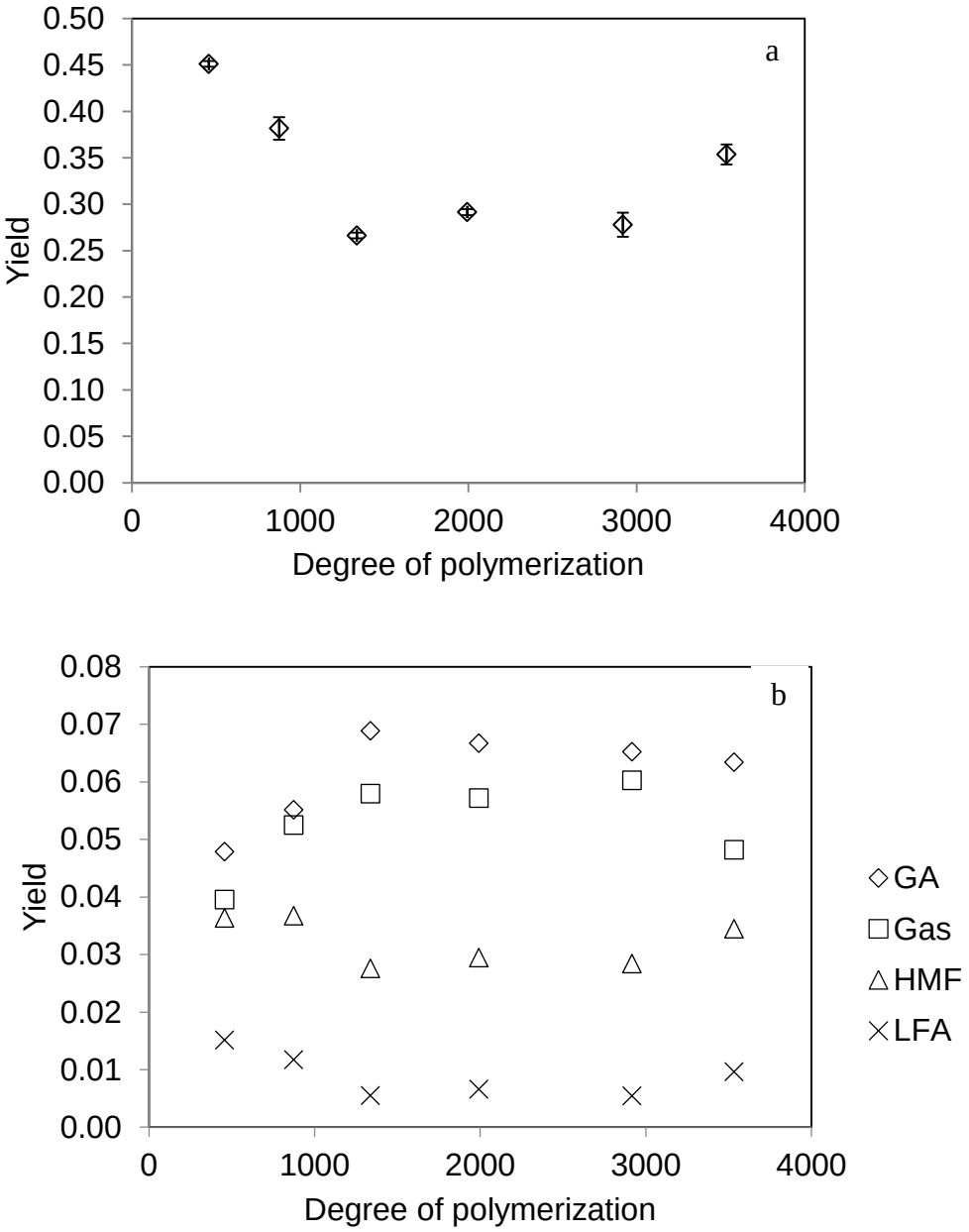


**Figure 1.2** Yield for individual components as a fraction of total measured peak area. 1.1a (levoglucosan) and 1.1b (GA, gas, HMF, LFA). Experiments were performed in duplicate. Yield given as the peak area of compound divided by total peak area..

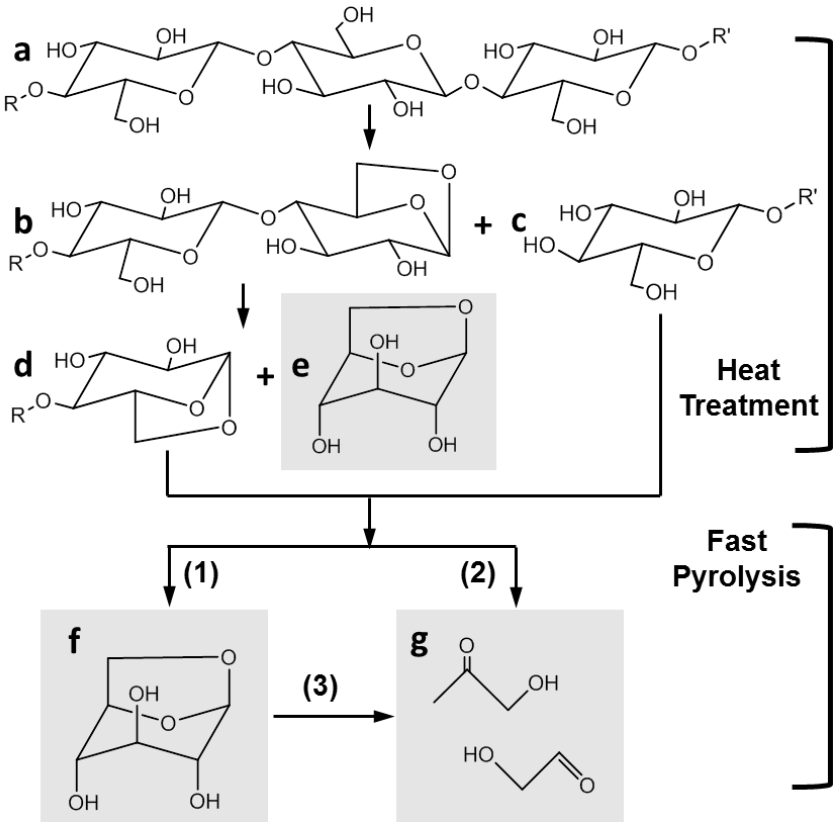


**Figure 1.3** Levoglucosan formation pathway with side reactions to form glycolaldehyde and acetol (Meng).

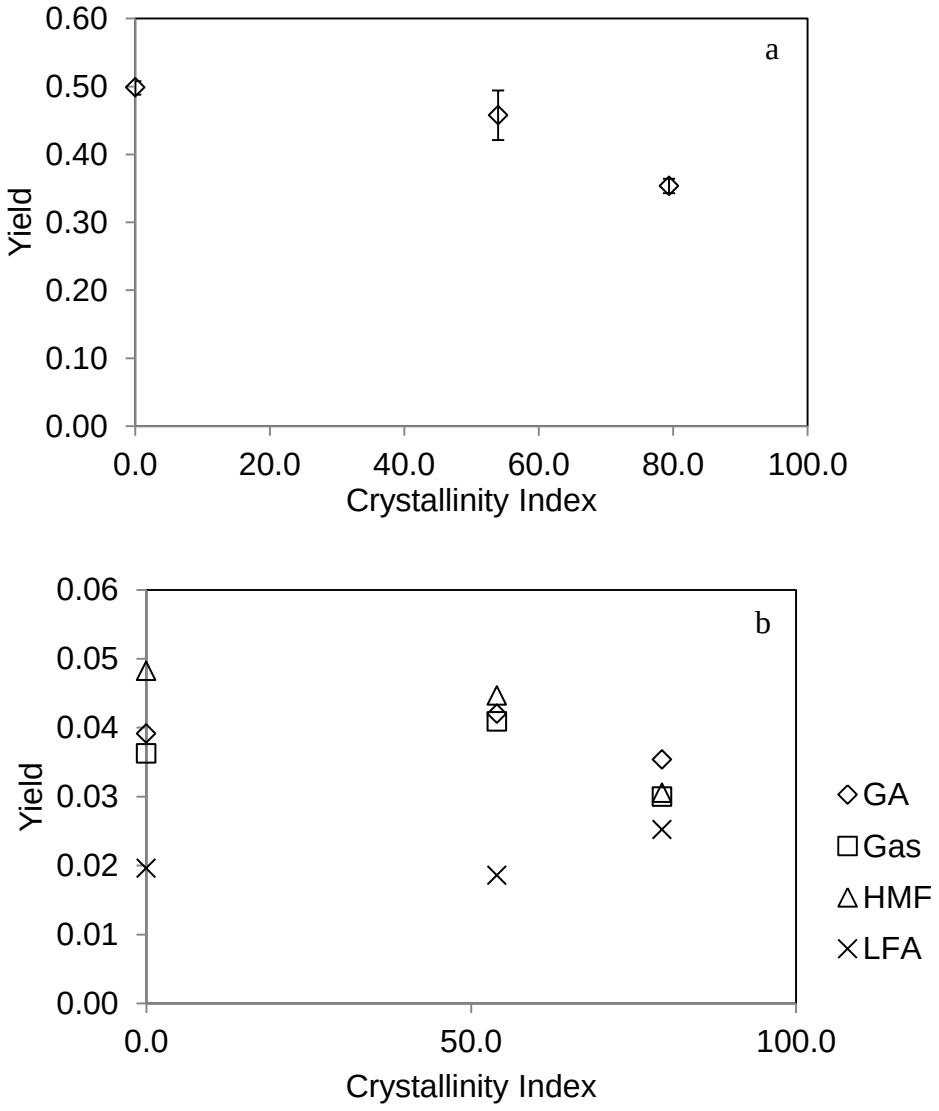


**Figure 1.4** Yield for individual components as a fraction of total measured peak area. 1.4a (levoglucosan), 1.4b (GA, gas, HMF, LFA). Experiments were performed in duplicate. Yield given as the peak area of compound divided by total peak area.

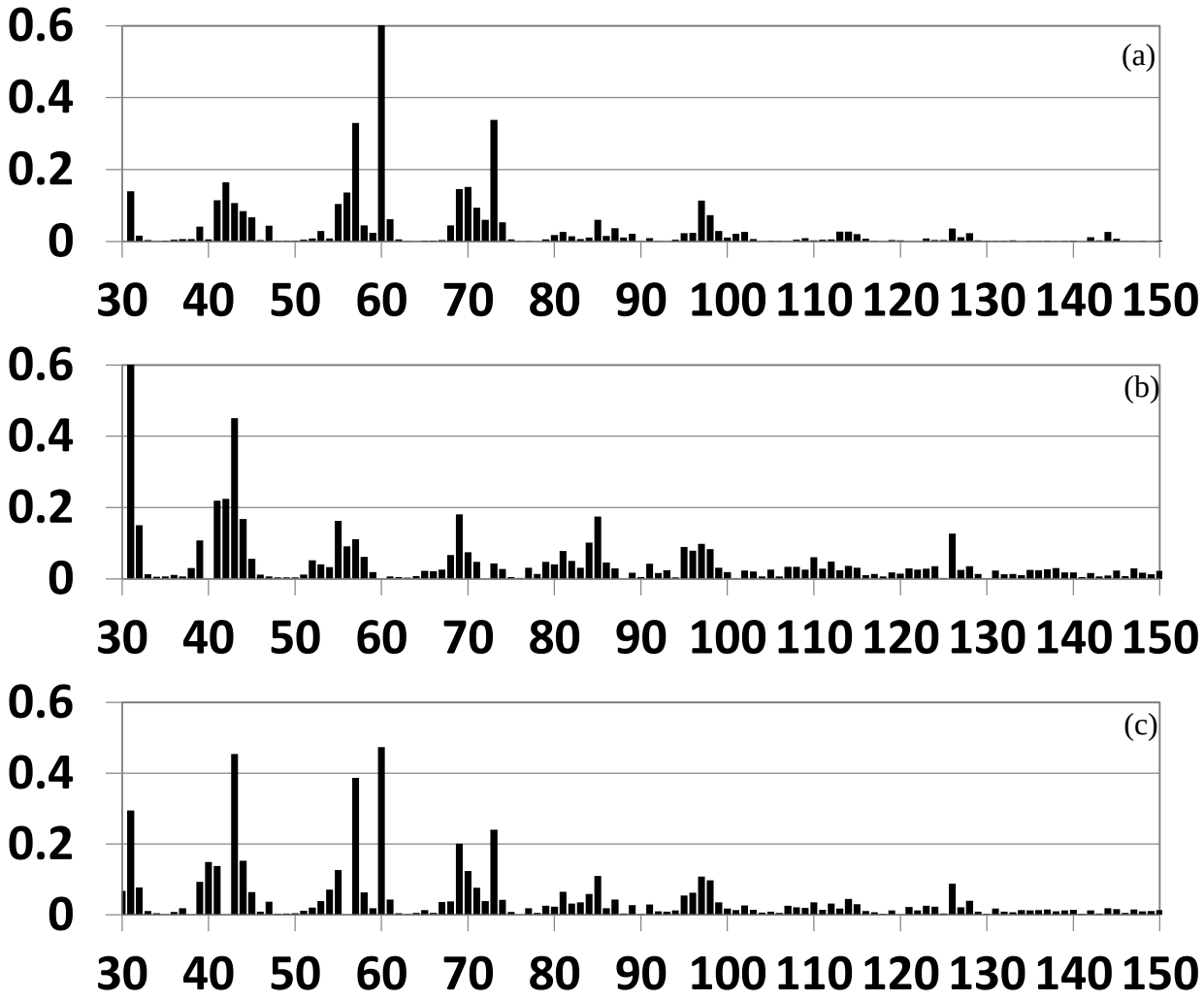


**Figure 1.5** Mass spectra for designated principal components from MBMS analysis. a (PC-1), b (PC-2), c (PC-3).

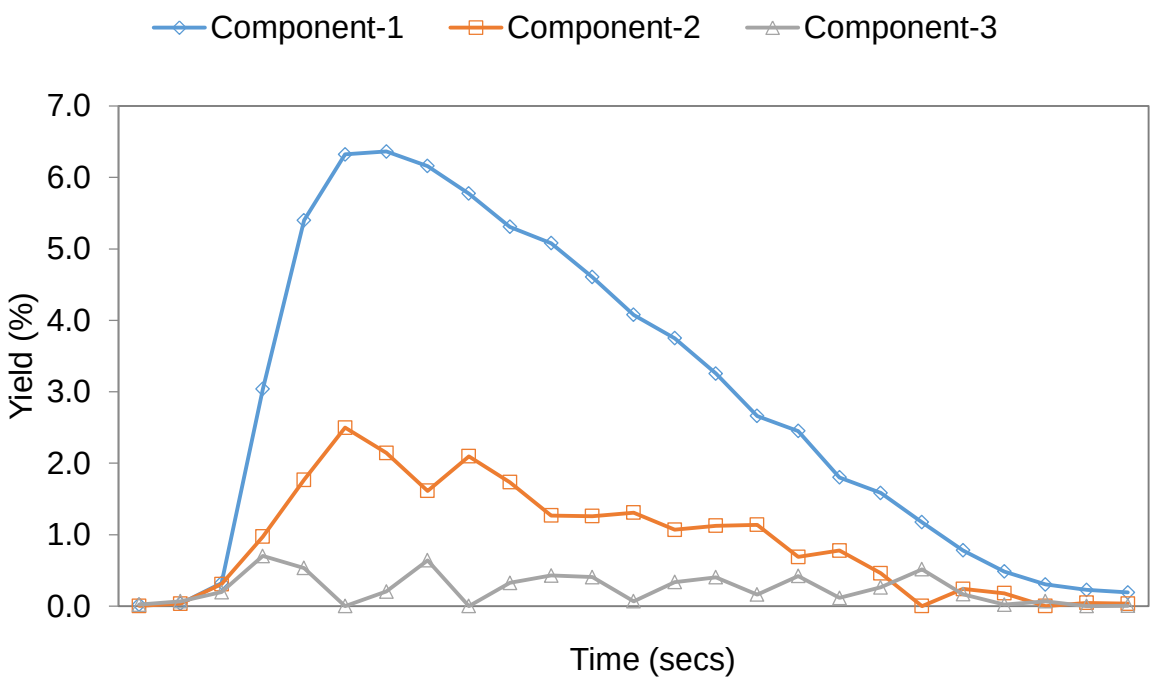


**Figure 1.6** Comparison of principal components over time for FP-Control.

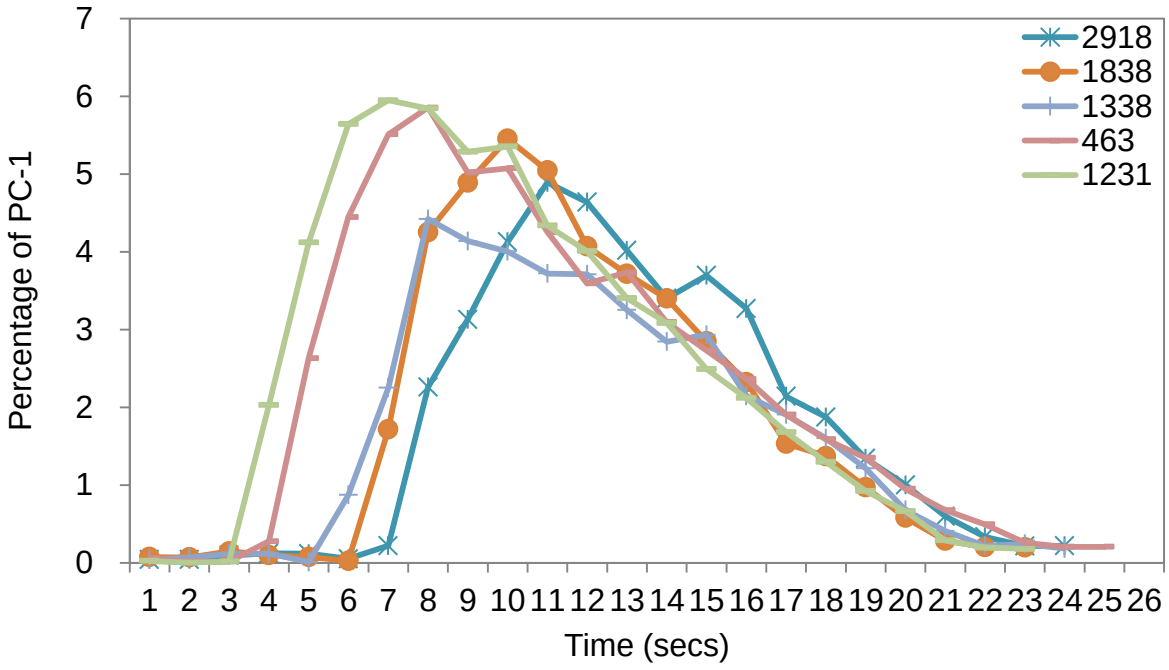


**Figure 1.7** Progression of PC-1 over time for varied DP samples.

**Table 1.1** Physical characteristics of cellulose samples for PY-GC/MS.

| Sample Name | Crystallinity Index[a] | Degree of polymerization[b] | Fiber Width (mm)[c] | ± |
|---|---|---|---|---|
| FP-Control | 79.4 | 4016 | 21.5 | 0.331 |
| FP-CrI-01 | 54.0 | 4000 | | |
| FP-CrI-02 | 0.0 | 4004 | | |
| FP-DP-01 | 83.4 | 457 | 19.5 | 0.253 |
| FP-DP-02 | 83.8 | 875 | 19.8 | 0.239 |
| FP-DP-03 | 83.5 | 1338 | 20.4 | 0.261 |
| FP-DP-04 | 83.2 | 1993 | 20.8 | 0.278 |
| FP-DP-05 | 79.9 | 2918 | 20.8 | 0.282 |
| FP-DP-06 | 82.9 | 3535 | 20.1 | 0.268 |

[a]: Amorphous subtraction crystallinity method.

[b]: BCA reducing ends measurement.

[c]: Measured by FQA.

**Table 1.2** Proximate analysis data from TGA for select samples.

| Sample Name | Moisture (%) | Volatile Matter (%) | Fixed Carbon (%) | Ash (%) |
|---|---|---|---|---|
| FP-Control | 2.57 | 97.14 | 0.00 | 0.31 |
| FP-DP01 | 2.15 | 95.93 | 1.92 | 0.00 |
| FP-DP04 | 2.77 | 89.73 | 6.97 | 0.53 |
| FP-DP06 | 2.72 | 94.45 | 2.15 | 0.68 |
| FP-CrI01 | 4.19 | 88.53 | 5.36 | 1.93 |
| FP-CrI03 | 5.50 | 90.63 | 3.87 | 0.00 |

**Table 1.3** Yields of compounds identified in Py-GC-MS experiments. Yields determined by compound peak area divided by total peak area. Displayed values are the average of two runs.

| Compound | FP-Control | FP-CrI01 | FP-CrI02 | FP-DP01 | FP-DP02 | FP-DP03 | FP-DP04 | FP-DP05 | FP-DP06 |
|---|---|---|---|---|---|---|---|---|---|
| Gas ($H_2O$, $CO_2$, CO) | 3.00 | 4.09 | 3.63 | 3.95 | 5.25 | 5.79 | 5.72 | 6.02 | 4.82 |
| Glycolaldehyde (GA) | 3.54 | 4.20 | 3.91 | 4.78 | 5.51 | 6.89 | 6.67 | 6.52 | 6.34 |
| Acetic Acid (AA) | 0.29 | 0.34 | 0.30 | 0.40 | 0.56 | 0.90 | 0.83 | 0.85 | 0.50 |
| Acetol | 1.84 | 1.82 | 1.51 | 2.03 | 2.76 | 4.17 | 4.17 | 2.73 | 3.06 |
| Succindialdehyde | 0.49 | 0.81 | 0.56 | 0.99 | 1.51 | 2.65 | 2.39 | 2.51 | 1.79 |
| Furfural | 1.05 | 1.31 | 1.26 | 1.17 | 1.32 | 1.31 | 1.27 | 1.25 | 1.22 |
| 3-Furan Methanol | 1.03 | 1.46 | 1.26 | 1.61 | 2.02 | 2.56 | 2.47 | 2.52 | 2.13 |
| 2-Furan Methanol | 0.35 | 0.57 | 0.50 | 0.54 | 0.64 | 0.75 | 0.71 | 0.73 | 0.70 |
| HMC | 0.87 | 1.14 | 0.82 | 1.19 | 1.51 | 1.93 | 1.84 | 1.87 | 1.43 |
| DGP | 1.87 | 1.56 | 1.51 | 1.50 | 1.42 | 1.08 | 1.04 | 1.03 | 1.26 |
| 5-HMF | 3.06 | 4.47 | 4.82 | 3.63 | 3.67 | 2.76 | 2.94 | 2.84 | 3.44 |
| Anhydroxylopyranose | 2.31 | 2.60 | 3.09 | 1.58 | 1.76 | 1.26 | 1.31 | 1.15 | 1.98 |
| Levoglucosan (pyranose) | 56.60 | 45.77 | 49.87 | 45.10 | 38.16 | 26.63 | 29.15 | 27.79 | 35.35 |
| Levoglucosan (furanose) | 2.52 | 1.86 | 1.96 | 1.51 | 1.17 | 0.55 | 0.66 | 0.54 | 0.96 |

# CHAPTER 2

## The Effects of Calcium Formate for In-situ Hydrogen Generation During Fast Pyrolysis of Woody Biomass

### 1. Introduction

Biomass has long been used as a heating source via combustion; however, higher value products can be obtained from it through other conversion pathways (Czernik and Bridgwater). The benefit of using biomass as an energy source is that it can be converted into liquid fuels, unlike other renewable resources such as solar, wind, and geothermal. The potential use of biomass as a liquid fuel source has been the driving factor for the past few years of research in this field and will continue to push research in the future (Oasmaa and Czernik). Fast pyrolysis, based on thermal conversion, is a promising method that can be used to transform lignocellulosic biomass into crude bio-oil, which is potentially compatible in a petroleum refinery (Bridgwater "Production of High Grade Fuels and Chemicals from Catalytic Pyrolysis of Biomass"). This process offers versatility in that many types of biomass, including forest resources, agricultural residue, energy crops, and industrial residue, can be used to produce fuels and chemicals. In contrast, biochemical conversion process suffers from the recalcitrant nature of biomass such as its high degree of lignification and crystalline structure, especially for softwood (Himmel et al.). Although a high yield of bio-oil can be achieved from the fast pyrolysis process using various biomass types, several challenges need to be resolved before the crude bio-oil can be utilized. Bio-oil is unstable, acidic, and contains about 35% oxygen content. These properties of bio-oil have restricted its

use in various applications and thus, it needs to be substantially deoxygenated into a mixture of organic molecules. In addition, it needs to be stable during storage and shipment. Current bio-oil sees a rapid increase in viscosity with storage time, which lasts from a few weeks to months (Venderbosch et al.). The presence of highly oxygenated compounds is one of the reasons for the unstable nature of bio-oil. Whether it is for the production of transportation fuels or heating source, the biggest hurdle is the amount of oxygen present. There is a challenge in retaining carbon in the final product, while reducing the amount of oxygen during the fast pyrolysis and upgrading process, due to the excessive CO, $CO_2$ and char formation. The proposed process retains more carbon by following the red pathway, as the oxygen is reduced during the fast pyrolysis. Subsequent upgrading would remove a smaller amount of carbon.

The process of reducing the oxygen, deoxygenation, in bio-oil has been a major area of research in recent years (Meng et al.; Ko et al.; Donnis et al.). Oxygen can be removed from bio-oil through two primary pathways, hydrotreating or catalytic conversion (Elliott; Bridgwater "Catalysis in Thermal Biomass Conversion"). Hydrotreating requires pure hydrogen to be used at high pressure to remove oxygen as $H_2O$, $CO_2$, and CO (Zhang et al.). Hydrogen is often produced by reforming natural gas in external facilities. This causes hydrogen to become more expensive and also less renewable. Hydrotreating also requires high pressure to be utilized, which necessitates modified equipment to handle the non-atmospheric pressures. Catalysts can be utilized to crack the bio-oil (Nava et al.; Adjaye and Bakhshi). The catalysts used tend to remove oxygen as CO or $CO_2$, which results in significant loss of carbons (French and Czernik). These catalysts also use extremely

expensive precious metals such as platinum, which make this process less economically feasible. Catalysts also have issues with coke formation, and the coke needs to be burnt off to regenerate the catalyst, which increases the energy usage. A less prominent method of upgrading bio-oil is the use of chemicals during pyrolysis (Mukkamala et al.). Other work shows that in-situ hydrogen production can reduce the amount of light oxygenates in the bio-oil while producing more aromatic and cycloalkane compounds (Fisk et al.).

This study aims to utilize calcium formate as an additive to fast pyrolysis biomass in prodder to produce in-situ hydrogen. This reactive hydrogen could react with oxygen in the pyrolysis vapors and be removed as water, thus decreasing the oxygen content of the organic fraction in the final bio-oil. Figure 2.1 shows the proposed reactions to take place during pyrolysis and the included recovery process. The calcium formate can be recycled and reformed simply with water and heat, thus significantly reducing the potential cost for this process.

## 2. Materials and Methods

### 2.1 Biomass samples

Loblolly pine chips, including bark, were ground to a 40-60 mesh particle size and used as the base material. Six samples were prepared in total with varied mixing techniques and concentrations. LP-Raw is the control, loblolly pine. LP-DMCF-1:1 is loblolly pine mixed with additive calcium formate (Sigma-Aldrich ≥99.0%); one part calcium formate, one part loblolly pine. LP-DMCF-1:5 has five parts loblolly pine to one part calcium formate. The DMCF series is loblolly pine physically mixed with calcium formate powder. LP-

WMCF-1:2D is loblolly pine soaked in a solution containing calcium formate in water, one part of calcium formate were added for every two parts of loblolly pine. LP-WMCF-1:1 is 50g $Ca(OH)_2$ (Sigma-Aldrich ≥96%) in water with 100g loblolly pine powder, then 50g of formic acid (Sigma-Aldrich ≥95.0) was added to produce calcium formate. LP-WMCF-1:2 is the same, except 100g of formic acid was added. The wet samples were allowed to react for one hour and left in an oven to dry overnight.

## 2.2 Fast pyrolysis

Fast pyrolysis experiments were conducted on a lab-scale reactor shown in Figure 2.2. The system consists of three primary regions, feeding, reactor, and cooling. 150 grams of sample were placed inside the hopper where they were gravity-fed onto a screw feeder into the reactor at 30 rpms. 6L/min of $N_2$ (99%) was added onto the screw feeder to aid in feeding the biomass. The reactor used was a fluidized bed design and 43mm diameter. Prior to heating, 200g of sand (VWR) was added to the reactor as a fluidizing medium. A second stream of $N_2$ was introduced at the bottom of the reactor in order to fluidize the sand bed. The two $N_2$ streams ensure that there is no oxygen in the system and are vital for keeping the process continuous. The reactor and cyclone char collector are housed within a 2 piece heating jacket that is temperature controlled by the K-type thermocouple placed in the sand bed. The temperature within the reactor is maintained at 500-510°C by adjusting the feeding rate of biomass. At the exit of the reactor is a char cyclone type char collector to remove char, sand, and any heavy solids, while allowing the vapors to pass through and exit to the condensers. The collections section of the system includes two condensers in series followed

by an electrostatic precipitator (ESP). The condensers are cooled by water at 4°C and at the bottom of the first condenser is a collection pot where the fraction BOC (bio-oil condenser) is taken. At the exit of the second condenser, the vapors are precipitated by the ESP at 13kV. This removes any organic compounds not condensed earlier and they fall into a collection jar under the ESP and the bio-oil collected here is called BOP (bio-oil precipitator). Non-condensable gases pass through and are cleaned further by two scrubber jars filled with distilled water. The clean gas is then vented to the outside atmosphere.

## 2.3 Analyses

### 2.3.1 Thermogravimetric analysis (TGA)

TGA was performed on a TA Instruments Q500 thermogravimetric analyzer. The temperature was increased from 25-900°C at a heating rate of 50°C/min. The analysis was performed in nitrogen and then switched to air after 30 min at 900°C to determine the ash content, as per the ASTM E1131-08 method. The TGA and DTG curves were measured for onset points and maximum weight loss temperature.

### 2.3.2 Water content

The water content was measured with a Automatic Volumetric Karl Fischer Titrator (Schott) using HYDRANAL Solvent E (Sigma-Aldrich) and HYDRANAL TITRANT 5E (Sigma-Aldrich). The system was calibrated with DI water prior to analysis and the average of three measurements was reported.

### 2.3.3 Ultimate Analysis

Carbon, hydrogen, and nitrogen contents were measured by a 2400 Series II CHN Elemental Analyzer (Perkin Elmer) by the Soil Science department at NC State. Approximately 7mg of sample were used for each measurement and the analyses were performed in triplicate to ensure accuracy. Oxygen content was not directly measured, but was calculated by the difference. Calcium content was also measured in this laboratory by a Dionex DX-500 ion chromatography system. The calcium measurements were performed in duplicate, separately from the CHNO.

### 2.3.4 Gas Chromatography/Mass Spectrometry

Gas chromatography/mass spectrometry analyses of the pyrolysis bio-oil were performed on a Finnigan Polaris Q Plus system. The MS detector was set at a full scan mode with a mass to charge range from 10 to 450 amu. Standard electron impact (EI) ionization at 70 eV was employed and the ion source temperature was 200 °C. The GC column used for separation was a DB-1701 column 60 m × 0.25 mm with 0.25 μm film thickness. The GC oven temperature was initially held at 45 °C for 4 min, then ramped at 3 °C/min to 280 °C, and held at 280 °C for 15 min. The injector and detector temperatures were set at 250 and 280 °C, respectively. The injector split ratio was fixed at 30:1. High purity helium (99.99%) was employed as the GC carrier gas at a flow rate of 38 cm/min, and duplicate tests were performed for each analysis. Compounds were identified based on comparative analysis of references, known standards, and the NIST 2008 library.

## 3. Results and Discussion

### 3.1 Biomass Characterization

TGA was used to investigate some of the thermal and physical properties of the biomasses. Figure 2.3 shows the decomposition of all biomass samples to 900°C. The initial loss is due to water as residual moisture is driven out of the samples. There is a sharp increase in weight loss at 413°C which corresponds to the degradation of cellulose and some left over hemicelluloses. Additionally, for the formate samples, this is where calcium formate decomposes into calcium carbonate ($CaCO_3$), hydrogen ($H_2$), and carbon monoxide (CO). The following peaks are between 554°C and 797°C, and as can be seen, they are not present in LP-Raw, thus they should be a product of the calcium formate. Indeed, these peaks correspond to the decomposition of calcium carbonate into calcium oxide (CaO) and carbon dioxide ($CO_2$). The final peak at 900°C is the introduction of air into the system to leave only the ash afterwards. In the LP-Raw sample it can be seen to slowly degrade after the 413 peak which is the degradation of lignin over a wide range of temperatures.

### 3.2 Bio-oil Characterization

A visual comparison between the bio-oils produced revealed that the BOC (oil from condenser) was identical for LP-Raw, LP-DMCF-1:1, LP-DMCF-1:2, LP-DMCF-1:5, and LP-WMCF-1:2D; they were a dark brown color. However, the BOC oils from LP-WMCF-1:1 and LP-WMCF-1:2 were very different, they were very aqueous and their color was more yellow, almost amber; the difference is noted in Figure 2.4. This indicates that there is some very different chemistry occurring when the wet-mixing is used to introduce the calcium

formate. The BOP oils were all a dark-brown viscous color with no visual differences between them.

The overall oil yield gives little information about the quality of the additive due to the high concentrations used. Table 2.1 expectedly shows that the oil yield decreases as the concentration of calcium formate increases, with LP-Raw having the highest oil yield at 67.55%. However, it also shows that on a per biomass basis; that is, considering only the loblolly pine powder in each sample, several formate samples showed an increased yield. The increase in yield for LP-DMCF-1:1 and LP-WMCF-1:1 could be due to the high amount of formate salt in these samples, some could have blown through the char collector and ended in the oil. It may have also come from an increase in water produced via the calcium formate decomposition. This "reaction water" would add to the total yield, but not be included in the base biomass. The percent of organics was also reported by removing the water from the bio-oil. The only two samples that showed improved organics yields on a per biomass basis were the samples with dry mixing. As expected, the char content increased significantly when calcium formate salt was added, but the gas remained relatively constant at 21-23% with the exception of LP-DMCF-1:1.

The water content measurements provided interesting results, which could explain the difference in appearance and are shown in Figure 2.5. Dry mixing of calcium formate with loblolly pine did not show any change in water content of the bio-oil, it remained close to 37% for the BOC oil and 7% for the BOP oil. However, there was a significant increase in water content of the BOC oils for the wet-mixed samples. The water content increased from 37% for LP-Raw to over 73% for LP-WMCF-1:2. This increase is significant, even

considering that there may be a slightly increased water content of the starting biomass during the preparation process. This possible small increase cannot account for large increase in water content of the wet-mixed samples. LP-WMCF-1:2D shows an increase in water content, but not as much as the wet-mixed samples which were produced via a reaction. This shows that a biomass samples that were prepared by the calcium hydroxide and formic acid reaction have an additional mechanism to produce water, it is not simply the location of the final calcium formate. It is possible the reaction that takes place during the preparation of these samples acts as a pretreatment method to allow the biomass to be broken down more easily in the reactor, thus producing more small products such as water.

As there may be some blow-through of sand/char into the bio-oil collection pots through the cyclone, the calcium content of biomass, char, and both bio-oils were measured in Figure 2.6. Expectedly, the calcium content was increased, with LP-DMCF-1:5 having the least and LP-DMCF-1:1 containing the most. It can be seen that the vast majority of the calcium was maintained in the char and collected in the char collector. However, a slight amount has made it through to the BOC oil in LP-WMCF-1:2 and 1:2D. This is not considered to be significant due to the low amount, <0.75wt%. Even less Ca made it into the BOP oil, the maximum is 0.20wt% for WMCF-1:2.

A sample GC/MS chromatogram is shown in Figure 2.7, with the corresponding primary peaks, retention times, and compound names given in Table 2.2. Semi-quantitative GC/MS results are displayed in Table 2.3 for BOC oil and Table 2.4 for BOP and give insight into what effect the calcium formate additive has on the quality of the bio-oil. It is noted here that GC/MS cannot identify all of the compounds present in bio-oil and this is

reflected in the percentage of the total peaks that were identified. For BOC oils, approximately 40% of all peaks were accounted for, however that dropped to around 30% for the BOP oils, which contain more phenolic and aromatic structures which are difficult to distinguish with the given tools. LP-WMCF-1:1 and 1:2 have a much lower glycolaldehyde content, 2.08wt% and 2.0wt% respectively, compared to LP-Raw, 9.72 wt%. Glycolaldehyde is a small oxygenate produced from woody biomass and it is a highly reactive compound, and could be a factor for the aging phenomenon of bio-oil. Additionally, these same samples show a much lower acetic acid content, 0.95wt% and 0.4wt% vs 2.64wt% for LP-Raw. Acetic acid is the primary acid in bio-oil and is likely the cause for high bio-oil acidity. Acetic acid catalyzes many aging reactions and thus is troublesome and ideal to be removed. Interestingly, the dry-mixed samples and wet-mixed with no reaction showed no discernable difference in these two compounds. Another abundant product of biomass pyrolysis is levoglucosan. This was also found to be less abundant for the samples in which a reaction took place. This information shows that the calcium formate is likely not effectively hydrogenating the biomass aerosols. The differences seen are due to acid/base reactions of the biomass preparation as an unintended pretreatment to the fast pyrolysis. The other compounds investigated also appeared to be in a lower abundance for these reaction samples as well, thus it could be possible that the calcium salt is catalyzing the pyrolysis reactions and the vapors are being broken down further into CO, $CO_2$, and $H_2O$. This is not ideal for pyrolysis, as we wish to obtain valuable chemicals from the bio-oil.

It was hypothesized that using calcium formate would decrease the final oxygen content by hydrogenating compounds during the pyrolysis process. Table 2.5 shows the

ultimate analysis and H/C and O/C ratios for the product bio-oils on a dry basis. The overall carbon content of the bio-oils decreased as calcium formate was added. Only LP-WMCF-1:1 and WMCF-1:2 showed a decrease in final oxygen content of bio-oil. These decreases were minimal, 46.21 to 45.73 and 44.94 respectively. These oils had significant decreases in oxygen content of BOP oil, 28.64 and 24.26, down from 32.70. However, they contained a higher amount of oxygen in the BOC oils. For the samples with a high amount of formate salt added (i.e DMCF-1:1, WMCF-1:1, and 1:2) there was an increase in O/C in the BOC oil. The H/C ratio for all BOC oils appears to be consistent and within experimental error. For the BOP oil, the WMCF-1:1 and 1:2 show a significant decrease in the O/C ratio. The O/C for LP-Raw was 0.54 and dropped to 0.44 for WMCF-1:1 and 0.36 for WMCF-1:2. Although this result was expected, it was expected for all samples, not only the samples in which a reaction occurred, thus this is deemed to be a result of the pretreatment method and not as a result of the hydrogenation of the vapors. This result is positive however, because it has shown that the oxygen content can be reduced significantly. It also appears that the oxygen from the reaction samples was selectively condensed as water. This led to an increase in O/C in the BOC oil, while a decrease in the O/C of the BOP oil.

## 4. Conclusions

Based on the results shown, the calcium formate is ineffective at decreasing the O/C ratio in bio-oil, as seen by the dry-mixed samples and wet-mixed sample with the formate salt dissolved. The wet-mixed samples with a reaction had much higher water content in BOC, lower amounts of nearly every compound, including glycolaldehyde, acetic acid, and

levoglucosan. These samples did however have a lower O/C ratio in the BOP oil, but it was accompanied by an increase in O/C in BOC oil. It appeared that these differences could be due to acid and base chemistry in the pretreatment method.

## 5. Acknowledgements

This study was supported by the United States Department of Agriculture National Needs Fellowship program (USDA NNF) and the Southeastern Partnership for Integrated Biomass Supply Systems (IBSS).

## REFERENCES


Czernik, S., & Bridgwater, A. (2004). Overview of applications of biomass fast pyrolysis oil. Energy & Fuels, 18(2), 590-598. doi: 10.1021/ef034067u

Oasmaa, A., & Czernik, S. (1999). Fuel oil quality of biomass pyrolysis OilsState of the art for the end users. Energy Fuels, 13(4), 914-921. doi:10.1021/ef980272b

Bridgwater, A. (1996). Production of high grade fuels and chemicals from catalytic pyrolysis of biomass. Catalysis Today, 29(1-4), 285-295. doi: 10.1016/0920-5861(95)00294-4

Himmel, M. E., Ding, S., Johnson, D. K., Adney, W. S., Nimlos, M. R., Brady, J. W., & Foust, T. D. (2007). Biomass recalcitrance: Engineering plants and enzymes for biofuels production. Science, 315(5813), 804-807. doi: 10.1126/science.1137016

Venderbosch, R. H., Ardiyanti, A. R., Wildschut, J., Oasmaa, A., & Heeresb, H. J. (2010). Stabilization of biomass-derived pyrolysis oils. Journal of Chemical Technology and Biotechnology, 85(5), 674-686. doi: 10.1002/jctb.2354

Meng, J., Park, J., Tilotta, D., & Park, S. (2012). The effect of torrefaction on the chemistry of fast-pyrolysis bio-oil. Bioresource Technology, 111, 439-446. doi: 10.1016/j.biortech.2012.01.159

Ko, C. H., Park, S. H., Jeon, J., Suh, D. J., Jeong, K., & Park, Y. (2012). Upgrading of biofuel by the catalytic deoxygenation of biomass. Korean Journal of Chemical Engineering, 29(12), 1657-1665. doi: 10.1007/s11814-012-0199-5

Donnis, B., Egeberg, R. G., Blom, P., & Knudsen, K. G. (2009). Hydroprocessing of bio-oils and oxygenates to hydrocarbons. understanding the reaction routes. Topics in Catalysis, 52(3), 229-240. doi: 10.1007/s11244-008-9159-z

Elliott, D. C. (2007). Historical developments in hydroprocessing bio-oils. Energy & Fuels, 21(3), 1792-1815. doi: 10.1021/ef070044u

BRIDGWATER, A. (1994). Catalysis in thermal biomass conversion. Applied Catalysis A-General, 116(1-2), 5-47. doi: 10.1016/0926-860X(94)80278-5

Zhang, X., Wang, T., Ma, L., Zhang, Q., & Jiang, T. (2013). Hydrotreatment of bio-oil over ni-based catalyst. Bioresource Technology, 127, 306-311. doi: 10.1016/j.biortech.2012.07.119

Nava, R., Pawelec, B., Castano, P., Alvarez-Galvan, M. C., Loricera, C. V., & Fierro, J. L. G. (2009). Upgrading of bio-liquids on different mesoporous silica-supported CoMo catalysts. Applied Catalysis B-Environmental, 92(1-2), 154-167. doi: 10.1016/j.apcatb.2009.07.014

ADJAYE, J., & BAKHSHI, N. (1995). Production of hydrocarbons by catalytic upgrading of a fast pyrolysis bio-oil .1. conversion over various catalysts. Fuel Processing Technology, 45(3), 161-183. doi: 10.1016/0378

French, R., & Czernik, S. (2010). Catalytic pyrolysis of biomass for biofuels production. Fuel Processing Technology, 91(1), 25-32. doi: 10.1016/j.fuproc.2009.08.011

Mukkamala, S., Wheeler, M. C., van Heiningen, A. R. P., & DeSisto, W. J. (2012). Formate-assisted fast pyrolysis of lignin. Energy & Fuels, 26(2), 1380-1384. doi: 10.1021/ef201756a

Fisk, C. A., Morgan, T., Ji, Y., Crocker, M., Crofcheck, C., & Lewis, S. A. (2009). Bio-oil upgrading over platinum catalysts using in situ generated hydrogen. Applied Catalysis A-General, 358(2), 150-156. doi: 10.1016/j.apcata.2009.02.006

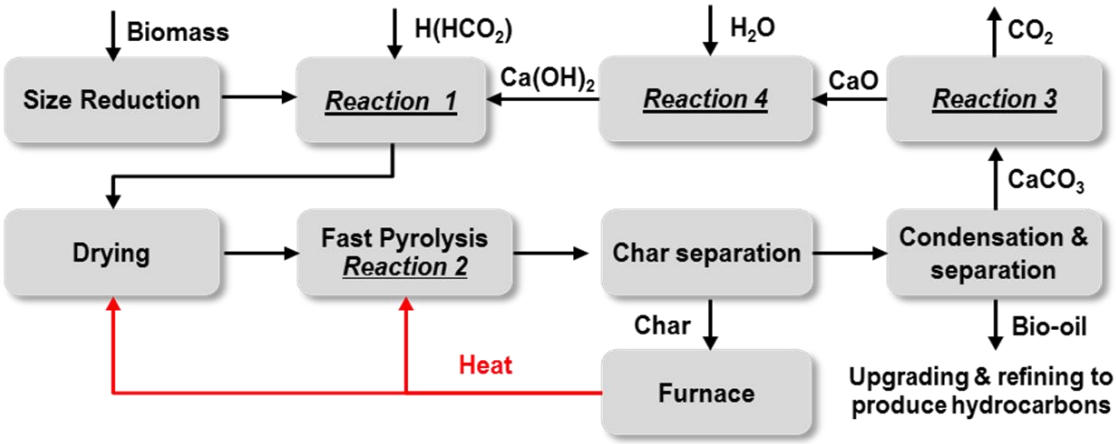


Reaction 1: $Ca(OH)_2 + 2H(HCO_2) \longrightarrow Ca(HCO_2)_2 + 2H_2O$

Reaction 2: $Ca(HCO_2)_2 \xrightarrow{\Delta} CaCO_3 + H_2 + CO$

Reaction 3: $CaCO_3 \xrightarrow{\Delta} CaO + CO_2$

Reaction 4: $CaO + H_2O \longrightarrow Ca(OH)_2$

**Figure 2.1** Flow diagram of proposed reactions and recycle streams of calcium formate during fast pyrolysis.

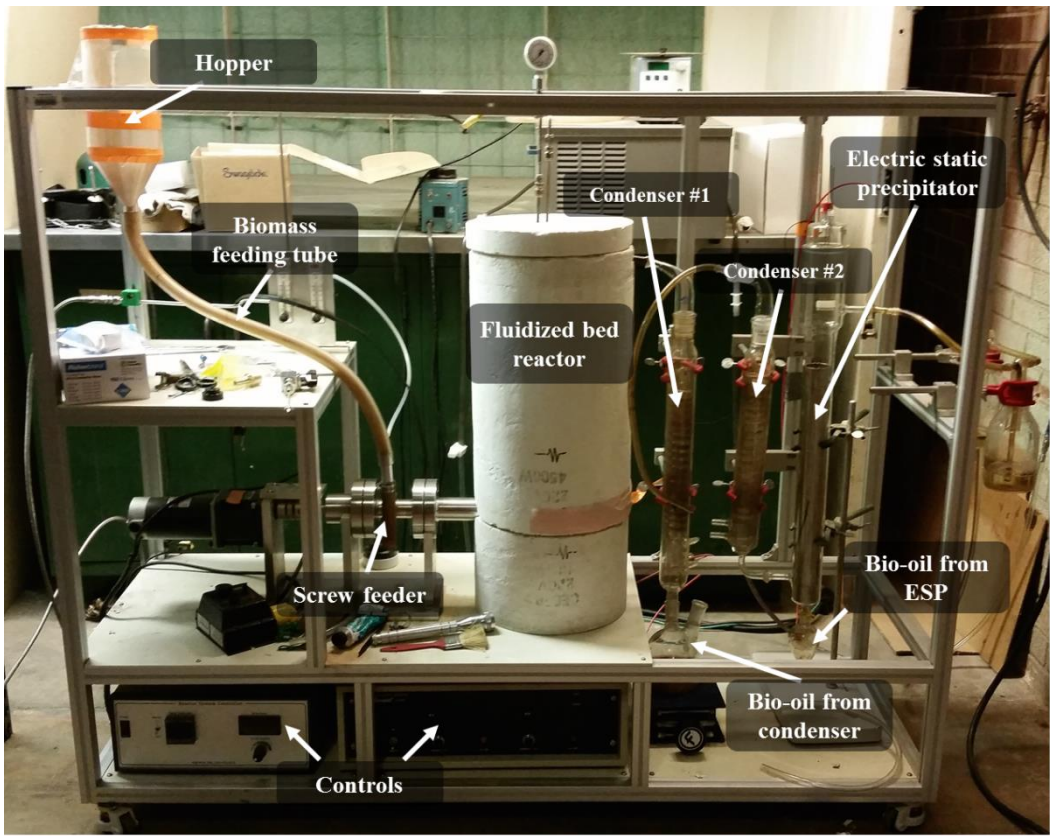


1

**Figure 2.2** Lab-scale fast pyrolysis plant used for experiments. Feeding system, furnace (containing reactor and char collector), and collection system are shown.

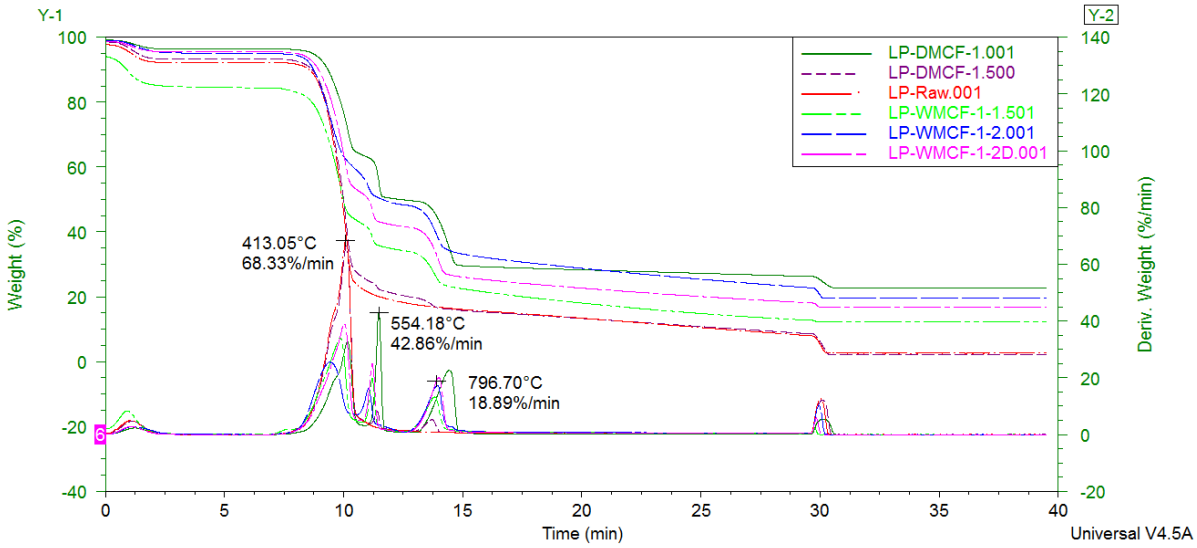


**Figure 2.3** TGA of all biomass samples. Heating rate- 50°C/min, final temperature 900°C.

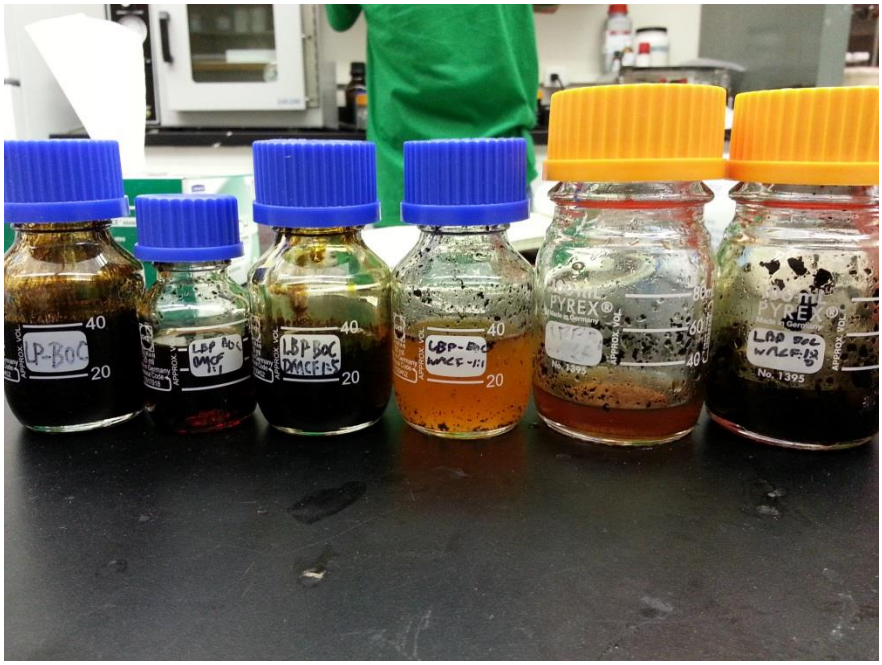


**Figure 2.4** BOC oils produced from fast pyrolysis. From left to right: LP, LP -DMCF-1:1, LP-DMCF-1:5, LP-WMCF-1:1, LP-WMCF-1:2, and LP-WMCF1:2D.

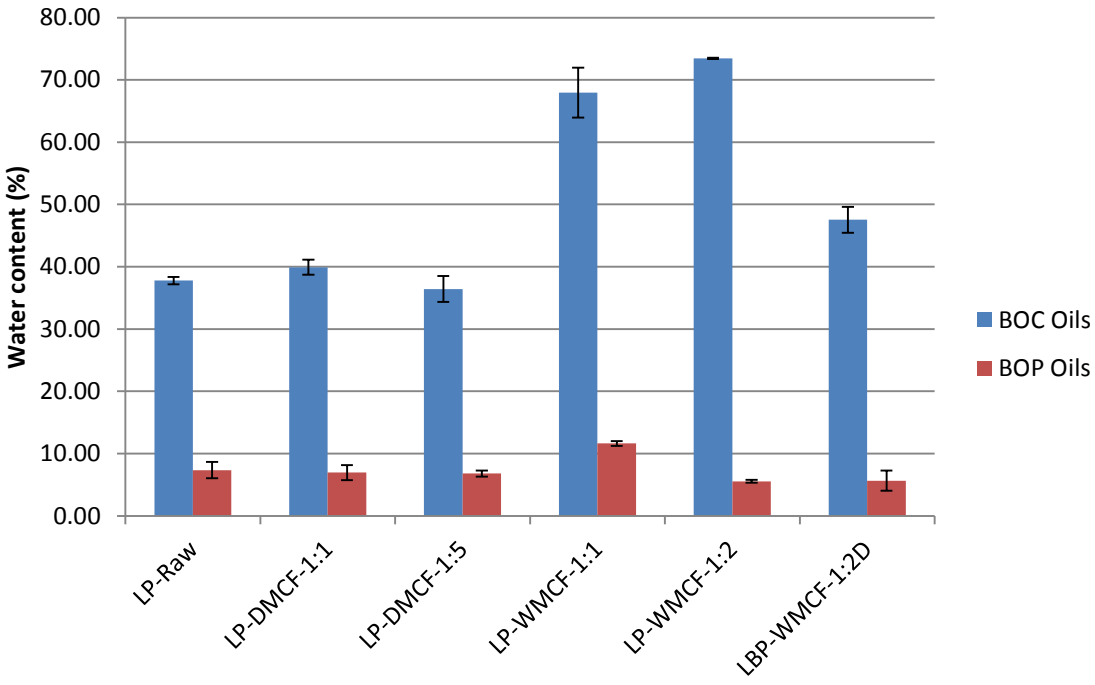


**Figure 2.5** Water content of bio-oil samples.

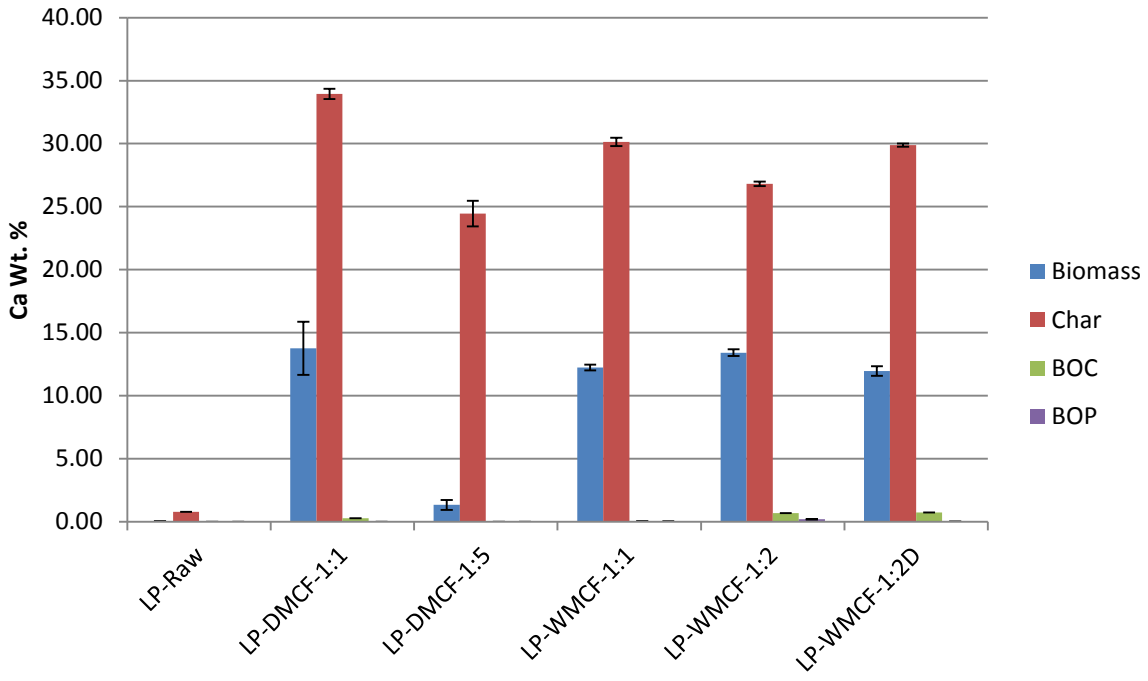


**Figure 2.6** Calcium content of all samples separated by fraction.

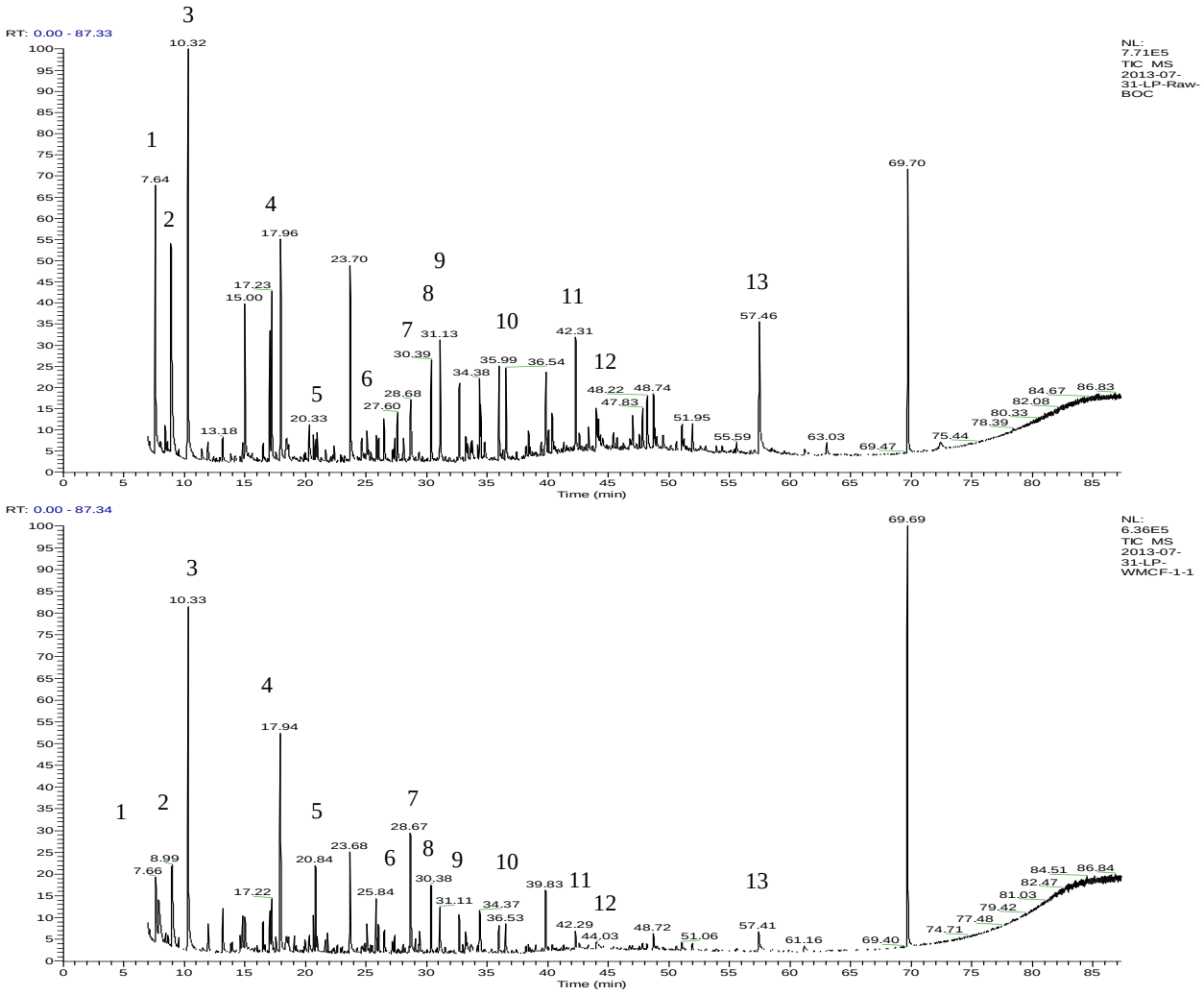


**Figure 2.7** GC/MS curves for BOC oil for LP-Raw (top) and LP-WMCF-1:1 (bottom). Peaks are numbered and identified in Table 2.2.

**Table 2.1** Amount of oil, char, gas, and organics based on [a]100g of air-dry sample and [b]100g of air-dry biomass.

| Sample Name | Oil[a] | Char[a] | Gas[a] | Organics[a] | Oil[b] | Organics[b] |
|---|---|---|---|---|---|---|
| LP-Raw | 67.55 | 9.52 | 22.93 | 47.79 | 67.55 | 47.79 |
| LP-DMCF-1:1 | 40.36 | 43.49 | 16.15 | 27.39 | 83.15 | 56.43 |
| LP-DMCF-1:5 | 57.70 | 21.89 | 20.41 | 41.31 | 69.63 | 49.85 |
| LP-WMCF-1:1 | 40.93 | 35.58 | 23.49 | 16.13 | 84.20 | 33.18 |
| LP-WMCF-1:2 | 28.62 | 48.06 | 23.32 | 9.95 | 58.91 | 20.47 |
| LBP-DMCF-1:2D | 44.72 | 32.89 | 22.39 | 26.98 | 68.03 | 41.04 |

**Table 2.2** List of peak numbers, compound names, and retention times.

| Peak Number | Compound Name | Retention Time (mins) |
|---|---|---|
| 1 | Glycolaldehyde | 7.69 |
| 2 | Acetic Acid | 8.94 |
| 3 | Acetol | 10.31 |
| 4 | Furfural | 17.98 |
| 5 | 2-methyl-2-Cyclopenten-1-one | 20.85 |
| 6 | 2,4-dimethyl-Furan | 25.84 |
| 7 | 3-methyl-1,2-Cyclopentanedione | 28.69 |
| 8 | Phenol | 30.42 |
| 9 | Guaiacol | 31.19 |
| 10 | p-Cresol | 36.06 |
| 11 | T-butyl phenol | 42.31 |
| 12 | HMF | 44.02 |
| 13 | Levoglucosan | 57.51 |

**Table 2.3** Major compounds detected by GC/MS in BOC.

| Compound Name | LP-Raw | LP-DMCF-1:1 | LP-DMCF-1:5 | LP-WMCF-1:1 | LP-WMCF-1:2 | LBP-DMCF-1:2D |
|---|---|---|---|---|---|---|
| Glycolaldehyde | 5.37 | 4.89 | 5.03 | 2.55 | 2 | 4.16 |
| Acetic Acid | 6.21 | 5.97 | 6.17 | 4.57 | 1.6 | 5.95 |
| Acetol | 7.26 | 7.41 | 7.37 | 9.28 | 11.4 | 8.62 |
| Furfural | 4.78 | 4.97 | 4.57 | 9.11 | 11.58 | 5.25 |
| 2-methyl-2-Cyclopenten-1-one | 0.33 | 0.7 | 0.44 | 2.24 | 3.84 | 0.84 |
| 2,4-dimethyl-Furan | 0.54 | 0.61 | 0.59 | 1.57 | 2.79 | 0.82 |
| 3-methyl-1,2-Cyclopentanedione | 1.71 | 2.07 | 1.73 | 4.42 | 5.38 | 3.85 |
| Phenol | 1.35 | 1.46 | 1.82 | 1.88 | 2.08 | 1.67 |
| Guaiacol | 2.27 | 2.88 | 2.24 | 1.4 | 1.7 | 1.48 |
| p-Cresol | 1.7 | 2.17 | 1.55 | 0.81 | 0.5 | 0.87 |
| T-butyl phenol | 2.47 | 2.21 | 2.16 | 0.13 | 0.37 | 1.69 |
| HMF | 1.34 | 1.25 | 1.43 | 0.48 | 0 | 1.34 |
| Levoglucosan | 4.06 | 3.45 | 4.75 | 0.91 | 0.13 | 4.3 |
| Total | 39.39 | 40.04 | 39.85 | 39.35 | 43.37 | 40.84 |

**Table 2.4** Major compounds detected by GC/MS in BOP.

| Compound Name | LP-Raw | LP-DMCF-1:1 | LP-DMCF-1:5 | LP-WMCF-1:1 | LP-WMCF-1:2 | LBP-DMCF-1:2D |
|---|---|---|---|---|---|---|
| Glycolaldehyde | 0.62 | 0.48 | 0.64 | 0.16 | 0.02 | 0.26 |
| Acetic Acid | 1.24 | 1 | 1.23 | 0.28 | 0.02 | 0.88 |
| Acetol | 1.67 | 1.26 | 1.61 | 0.64 | 0.27 | 1.16 |
| Furfural | 2.81 | 2.37 | 2.65 | 2.86 | 2.58 | 2.47 |
| 2-methyl-2-Cyclopenten-1-one | 0.28 | 0.47 | 0.35 | 1.23 | 1.56 | 0.57 |
| 2,4-dimethyl-Furan | 0.45 | 0.42 | 0.56 | 1.24 | 1.52 | 0.78 |
| 3-methyl-1,2-Cyclopentanedione | 1.73 | 2.2 | 1.95 | 4.32 | 4.05 | 3.81 |
| Phenol | 1.38 | 1.18 | 1.39 | 1.35 | 1.46 | 1.19 |
| Guaiacol | 2.32 | 3.04 | 2.25 | 2.18 | 2.39 | 1.74 |
| p-Cresol | 2.19 | 2.53 | 1.88 | 1.58 | 1.66 | 1.13 |
| T-butyl phenol | 4.67 | 4.77 | 0.99 | 3.54 | 3.18 | 3.78 |
| HMF | 2.38 | 2.29 | 2.47 | 1.79 | 0.95 | 2.29 |
| Levoglucosan | 9.17 | 7.51 | 8.59 | 4.21 | 0.79 | 7.17 |
| Total | 30.91 | 29.52 | 26.56 | 25.38 | 20.45 | 27.23 |

**Table 2.5** Ultimate analysis and calcium content of bio-oil samples. Values are calculated on a dry basis.

| Sample Name | C | H | N | Ca | O | O/C | H/C |
|---|---|---|---|---|---|---|---|
| **BOC Oils** | | | | | | | |
| LP-Raw | 43.37 | 4.60 | 0.57 | 0.00 | 51.46 | 1.19 | 0.11 |
| LP-DMCF-1:1 | 38.80 | 4.27 | 0.57 | 0.49 | 55.86 | 1.44 | 0.11 |
| LP-DMCF-1:5 | 43.01 | 5.12 | 0.67 | 0.00 | 51.19 | 1.19 | 0.12 |
| LP-WMCF-1:1 | 29.79 | 4.24 | 0.76 | 0.18 | 65.03 | 2.18 | 0.14 |
| LP-WMCF-1:2 | 40.03 | 7.76 | 0.92 | 2.60 | 48.69 | 1.22 | 0.19 |
| LBP-WMCF-1:2D | 45.09 | 5.03 | 0.62 | 1.43 | 47.83 | 1.06 | 0.11 |
| **BOP Oils** | | | | | | | |
| LP-Raw | 60.42 | 6.54 | 0.33 | 0.00 | 32.70 | 0.54 | 0.11 |
| LP-DMCF-1:1 | 61.14 | 6.41 | 0.35 | 0.01 | 32.09 | 0.52 | 0.10 |
| LP-DMCF-1:5 | 59.98 | 6.48 | 0.29 | 0.01 | 33.25 | 0.55 | 0.11 |
| LP-WMCF-1:1 | 64.45 | 6.38 | 0.50 | 0.03 | 28.64 | 0.44 | 0.10 |
| LP-WMCF-1:2 | 68.15 | 7.04 | 0.33 | 0.21 | 24.26 | 0.36 | 0.10 |
| LBP-WMCF-1:2D | 60.80 | 6.43 | 0.31 | 0.03 | 32.43 | 0.53 | 0.11 |
| **Total** | | | | | | | |
| LP-Raw | 48.14 | 5.14 | 0.51 | 0.00 | 46.21 | 0.96 | 0.11 |
| LP-DMCF-1:1 | 44.08 | 4.78 | 0.51 | 0.38 | 50.25 | 1.14 | 0.11 |
| LP-DMCF-1:5 | 47.60 | 5.49 | 0.57 | 0.00 | 46.34 | 0.97 | 0.12 |
| LP-WMCF-1:1 | 34.32 | 4.52 | 0.73 | 0.16 | 60.27 | 1.76 | 0.13 |
| LP-WMCF-1:2 | 43.43 | 7.68 | 0.85 | 2.31 | 45.73 | 1.05 | 0.18 |
| LBP-WMCF-1:2D | 48.04 | 5.29 | 0.56 | 1.17 | 44.94 | 0.94 | 0.11 |

# CHAPTER 3

## Fast Pyrolysis of Lignin-Coated Biomass

### 1. Introduction

The valorization of secondary streams such as extracted tannins and Acetosolv lignin from Pinus radius is a key issue in the development of lignocellulosic biorefineries (De Wild, Huijgen and Gosselink). In the last decade, an intensive research activity was carried out on the valorization of technical lignins (Zakzeski et al.; de Wild, Reith and Heeres; Nowakowski et al.; Gosselink et al.), while the valorization of extracted tannins has been studied more recently (Feng et al.; Case et al.).

Urged by a need of diversifying its pool of technologies to produce renewable energy, Chile with its natural abundance of woody biomass supported the implementation of fast pyrolysis in the country. A fast pyrolysis process using a three-stage fluidized bed reactor system with a feed capacity of 10 kg/h was developed at the Unidad de Desarrollo Tecnológico, UDT (Wilkomirsky, Moreno and Berg). Fast pyrolysis, a thermochemical process that converts biomass into a useful liquid product, is currently of particular interest for fuel and chemical production (Xiu and Shahbazi). The valorization of technical lignins such as acid-extracted and Organosolv lignins are often considered due to their low sulfur content (Dondi et al.; Wyman), being a perfect candidate for the establishment of a cleaner valorization process. Previous works have proved the viability and feasibility of converting these lignins into a value-added chemicals source by showing the occurrence of high-value components (e.g., hydroxyacetaldehyde, acids, and phenolic monomers) in fast pyrolysis

bio-oil obtained from Acetosolv or Kraft lignin (Beis et al.), or Organosolv lignin (Patwardhan; Bai et al.). The concentration of these organic compounds depends on the nature of the lignocellulosic feedstocks (Mohan, Pittman and Steele), whose chemistry was altered during the extraction process (Wyman). However, the conventional fast pyrolysis of these extracted biopolymers presents numerous technical issues, in particular feeding problems due to their low fusion point, bed agglomeration, and low yield of highly oxygenated liquids (Nowakowski et al.; Case et al.; de Wild, Huijgen and Heeres). To overcome these technical barriers, several alternative pyrolysis modifications have been attempted, such as the co-feeding with alkaline catalyst or the use of a catalytic bed. For example, the addition of CaO helped decrease the oxygen content of bio-oil by reducing the concentration of levoglucosan in favor of the acetol (Y. Y. Lin et al.). The combined use of CaO and an olivine bed appeared to be beneficial, as it displayed a high liquid yield, 32 wt%, and favored the depolymerization of Acetocell lignins (Marion Carrier et al.). More recently, Li et al. (Li, Briens and Berruti) proposed the use of activated lignin bed to pyrolyze Kraft lignin in order to improve the bio-oil´s quality.

In this study, the coating of biomass particles with isolated lignin was proposed as an alternative method to the addition of catalysts. To fully understand the role of the coating preparation on product distribution and pyrolysis reactions, this study used both spectrometric and chromatographic techniques, 13C NMR and GC-MS, to respectively analyze the overall pyrolysis bio-oil and quantify its key-products obtained from raw biomass and coated materials pyrolysis degradation.

## 2. Materials and Methods

### 2.1 Materials and Preparation

#### 2.1.1 Feedstocks

Pinus radiata D. Don sawdust was provided by BSQ Ltda, a forest company located in Concepcion (Chile). The woody material was sieved to obtain a particle size in the range of 0.5-1.5 mm. The moisture content (MC) of the woody material was maintained at 10 wt%.

The acetic acid-extracted lignin (Acetosolv lignin) was prepared from the same Pinus radiata wood chips using an adaptation of the so-called Acetocell process (Berg, Fuentealba and Salazar). The woody material was delignified using an 87 wt% acetic acid solution at 185 °C for 2 hours. The dissolved lignin was precipitated by diluting the spent pulping liquor with water. The filtered lignin was washed with water multiple times. Since the pulping method is sulfur and sodium free, the Acetosolv lignin has low ash and contains almost no covalently bound sulfur in comparison to others extracted lignin originating from the kraft process (Wyman).

#### 2.1.2 Coated Feedstocks

A preparation method was developed to produce the coated feedstock with a uniform distribution of lignin. A solvent mixture of acetone (99.5%, Winkler) and water, four parts to one respectively, was utilized to fully dissolve the acetic-extracted lignin (up to 0.2 g/mL). A liquor to wood ratio of 8:1 was used to allow the slurry to be evenly mixed. The lignin was fully dissolved in the acetone/water mixture in 10 min with vigorous mixing (4000 rpm) via a mechanical stirrer. The pine powder was then added slowly over 10 minutes to ensure a

uniform mixture and allowed to mix for 4 hours. After mixing, the sample was left in a beaker, then covered, and allowed to soak overnight for further impregnation by lignin. The sample was then placed into a pan and placed in a fume hood to allow the solvent to evaporate, and then oven dried at 45°C for 2 h, and finally allowed to air dry for 48 h. The coated biomass was then sieved to the original 250-600 µm particle size.

2.2 Fast pyrolysis processing

The fast pyrolysis (FP) plant, Figure 3.1, can be divided into four sections: the biomass-feeding unit, the cylindrical furnace housing the bubbling fluidized bed reactor, one hot-gas filter as separation stage, and the condensation chain. The biomass feeding unit consisted of a hopper with a screw feeder, which introduced biomass (particle size 250–600 µm) at a feed rate of 0.1 ± 0.03 kg/h into the reactor. The hopper was maintained at a slight $N_2$ overpressure (±0.02 bar gauge, gas flow rate of 6 L/min) to prevent hot gas and product vapor pushing back from the reactor into the feeding system. A quartz bed was used as the heat carrier inside the reactor and fluidized using a $N_2$ gas flow rate of 9 L/min. Pyrolysis product vapors/aerosols and solid particles left the furnace via a heated pipe (maintained at 400 °C to prevent undesired intermediate condensation) before entering the hot gas filter at 400 °C. Once separated from solid particles, the aerosols/vapors underwent a condensation stage that consisted of a water-cooling tower at 4°C followed by an electrostatic precipitator set to 15 kV.

The bio-oil, product of interest, was collected from the condenser tower and precipitator and thus consisted of two single phases corresponding to the BOC and BOP

fractions. The char product was recovered from the hot-filter pot, while the non-condensable gases were purged to the atmosphere. Experimental runs were duplicated at 540 °C with a running time between 25 and 65 min.

All product yields ($Y_{char}$, $Y_{bio\text{-}oil}$, $Y_{organics}$, and $Y_{pyrolytic\ water}$) reported here were calculated on a dry mass basis (db, wt%) of the initial and dried biomass feed, $m_{biomass}(1-MC_0)$, as indicated by Equations 1-4. The bio-oil yield represents the total liquid product yield correcting for initial feed water content.

$$Y_{char}(db, wt.\%) = \frac{m_{char}(1-MC_{char})}{m_{biomass}(1-MC_0)} * 100 \quad (1)$$

$$Y_{bio-oil}(db, wt.\%) = \frac{m_{bio-oil}(1-MC_0)}{m_{biomass}(1-MC_0)} * 100 \quad (2)$$

$$Y_{organics}(db, wt.\%) = \frac{m_{bio-oil}(1-MC_{bio-oil})}{m_{biomass}(1-MC_0)} * 100 \quad (3)$$

$$Y_{pyrolyticwater}(db, wt.\%) = \frac{m_{bio-oil} * MC_{bio-oil} - m_{biomass} * MC_0}{m_{biomass}(1-MC_0)} * 100 \quad (4)$$

Where $m_{char}$, $m_{bio\text{-}oil}$, and $m_{biomass}$ are respectively the mass of recovered char, bio-oil and initial biomass. The gas yield was calculated by difference.

## 2.3 Analyses

### 2.3.1 Feedstock

Ultimate and proximate analyses were conducted on both feedstocks using respectively an elemental analyzer (Perkin Elmer 2400 Series II CHNS/O system) and a thermogravimetric analyzer (TA instruments Q500) using the ASTM E1131 standard procedure.

The surface of feedstock was analyzed using a single reflection attenuated total reflectance (ATR) FT-IR technique performed by a Platinum ATR Alpha instrument. A total of 24 scans between 4800-400 cm-1 were averaged at intervals of 4 cm-1. The software OPUS (Version 7) was used to normalize and display the spectra.

Compositional analysis was performed using a modified NREL method, which has been described elsewhere (Jones et al.). The determination of water, ethanol and hexane extractives within the raw Pinus Radiata was carried out following the NREL Laboratory Analytical procedure (Sluiter et al.).

An oven-dried sample mass of 0.1 g of 250-400 µm biomass was hydrolyzed with 72 wt% $H_2SO_4$ (Sigma-Aldrich) for 2 h, then diluted to 3% before being autoclaved at 120°C for 1.5 h. Hydrolysate was filtered and the liquid was analyzed by HPLC system (Agilent 1200, Agilent, Santa Clara, CA, USA) and UV-Vis spectrophotometer (Lambda XLS, Perkin Elmer, Waltham, MA, USA) for sugar and lignin analysis, respectively. The sugars, glucose, xylose, and galactose were detected and measured by ways of calibration curves obtained from standards, glucose (>99.5%, Sigma-Aldrich), xylose (>99%, Sigma-Aldrich), and galactose (>99%, Sigma-Aldrich). The solids were oven-dried at 105 °C and weighed to determine the insoluble lignin fraction.

The chemical structure of the lignin was determined by 1H NMR after complete acetylation of the material. The protocol of acetylation was an adaptation of the one proposed by Fernandez-Costas et al. (Fernandez-Costas et al.). Volumes of 5 mL of acetyl anhydride (99.2 %, Winkler) and 5 mL of pyridine (99.7 %, Winkler) were added to 52.5 mg of lignin in a dry acetylation vial, which was sealed and constantly stirred at 37 °C for 48 h. A volume

of 20 mL of cold distilled water was added to the mixture to remove the excess of pyridine and acetyl anhydride and subsequently precipitate the lignin. After the first centrifugation step at 15000 rpm for 4 min using an Eppendorf system (Model 5702), two additional clean-up steps were performed. The contents of the vial were finally dried at 40 °C for 48 h and milled with an agate mortar and pestle. Acetylated and non-acetylated lignins (~25 mg) were dissolved in 750 mL of deuterated methanol CD3OD-d4 (99.8 %, Merck). The spectra were collected on a Bruker Avance DSZ 400 MHz spectrometer at 23.5 °C, equipped with a BRUKER 5 mm PABBI 1H/D-BB Z-GRD liquid probe with a flip angle of 30°. The number of scan was 16 with an acquisition time of 6.3 s. Spectra were processed with Bruker TopSpin 3.1.

Finally, pictures of coated particles were taken using a scanning electron microscope (SEM) micrograph JEOL (JSM-6010LA) equipment using a magnification range of 22-2500 with a resolution of 0.28 nm.

### 2.3.2 Bio-oil

The water content of liquid fractions was determined using a Mettler Toledo V20 volumetric KF Titrator (ASTM E871) using the CombiTitrant 5 one-component reagent for volumetric Karl-Fisher titration (Merck) as titration reactant and dried methanol (max 0.003% H2O, Merck) as titration solvent.

Chemical functional groups of char and tarry fractions were determined using nuclear magnetic resonance (NMR), on a Bruker Avance DSZ 400 MHz spectrometer. The analysis of 13C NMR was acquired using ~140.0 mg tarry oil dissolved in 900 μL DMSO-d6 (99.8

%, Merck) or ~100.0 mg of char dissolved in 900 µL DMSO-d6 employing an inverse gated decoupling pulse sequence, 90° pulse angle, a pulse delay of 5 s for tarry oils, and 12 s for char. The 13C NMR spectra were acquired with a 90° pulse duration of 2.4 µs, and a sweep width of 25,000 Hz and 30,000 Hz for liquids and chars. Spectra were processed using Bruker TopSpin 3.1. The chemical shift values were calibrated on the solvent peak. The 13C NMR chemical shift assignment was determined based on previous works of Ben et al. (Ben and Ragauskas "Nmr Characterization of Pyrolysis Oils from Kraft Lignin").

The GC-MS analyses were performed using a Hewlett packard GC system (Model HP 6890Series) and a Hewlett packard Mass Selective detector (Model 5973). A column HP-5 60m x 0.25mm with a film thickness of 0.25 µm and operating conditions were based on following past procedures (Meng et al.). The heating program was an initial hold at 45 °C for 4 min, followed by a ramp to 280 °C at 3 °C/min, and finally held at 280 °C for 15 min. An aliquot of 0.2 g of bio-oil and 1 mL of internal standard (Fluoranthene, 98%, Aldrich) were added to a 10 mL volumetric flask that was completed with acetone (GC grade, Sigma-Aldrich) filtered through a 0.2 µm PTFE filter (Rephile). The volume injection was 1 µL and maintained by an autosampler. The mass spectrometer (MS) detector was used with a standard electron impact ionization chamber set at 70 eV with a temperature of 200 °C. The ions formed were separated via a quadrupole according their mass-to-charge (m/z) ratio in the range of 30-250 Da. Peaks were identified by the 2008 NIST library.

## 3. Results and Discussion

### 3.1 Feedstock

The initial characterization of the feedstocks was important to appreciate the efficiency of the coating method and the possible chemical and/or physical changes. The compositional analysis showed in Table 3.1 indicates that the lignin content was increased systematically and effectively. The starting biomass contained 32.78 wt% of native lignin, which was increased to 38.30 wt% in LI20 and to 46.83 wt% in LI40; thus corresponding respectively to an increase of 17% (LI20) and 43% (LI40) in lignin mass within the coated materials The moisture content remained constant for all samples between 3.97% and 5.61 wt% meaning the samples were effectively dried prior to being pyrolyzed. Although both ash content of virgin biomasses are low, 0.68 and 0.54 wt% for Pine and the isolated lignin respectively, a slight increase in ash content was observed for the coated preparations, 0.81 wt% for LI20 and 1.12 wt% for LI40. This result was attributed to the impurities present in the acetone solvent used during the preparation.

The chemical composition indicates that 7.74 wt% of the dry mass cannot be accounted for from the analysis results. Similar problems with respect to unclosed or overestimated mass balance were experienced in different studies (Park, Park and Kim; Oasmaa et al.). In some cases, authors attributed those deviations to unidentified or lost materials after acid hydrolysis of the biomass feedstock and/or the inaccuracy of the isolation method (Jung et al.; M. Carrier, A. Loppinet-Serani, et al.). In our case, the lignocellulose distribution falls within the literature range and the unclosed mass balance can be partially attributed to the fact that we did not report the concentration of arabinose nor mannose.

Lignin together with hemicelluloses and cellulose provide the lignocellulose biomass with a large and diverse distribution of functional groups. Although ATR-FTIR does not allow an accurate quantification of the functional groups (Zhou et al.), this technique can be used as qualitative screening. Clear spectral differences between feedstocks were observed in the regions of 3700-2700 and 1800-500 cm-1 (Figure 3.2). In the case of the isolated lignin, the respective strong bands at 1714, 1597, 1269 cm-1 , 1225 and 1127 cm-1 that are respectively assigned to the C=O stretching, aromatic skeletal vibration, combined C-O and C-C stretch and the aromatic C-H in-plane deformation in the guaiacyl ring, are characteristic of the coniferyl alcohol unit of softwood lignin (Kubo and Kadla). In addition, the bands centered at 1454 cm-1 and 2850 cm-1 corresponding respectively to the CH deformation - OCH3 aromatic and stretching vibration of C-H assigned to the OCH3 confirmed that numerous methoxy groups that belong originally to the guaiacol (G) unit remained in large proportion after the hydrolysis (Kubo and Kadla).

The efficiency of the acid hydrolysis of lignin was confirmed by two observations. Firstly, the presence of intense peaks at 1714 cm-1 and 1366 cm-1 attributed to the respective presence of carbonyl and hydroxyl groups indicates the cleavage of the aryl-ether bonds (Tejado et al.). Secondly, the absence of the band centered at 1315 cm-1 indicates that carbohydrates have been efficiently removed and their content remained low, 2.08 wt% (Table 3.1).

If the ATR-FTIR analysis qualitatively suggested the presence of side-chains with the detection of carbonyl groups, the use of 1H NMR analysis is a more suitable technique to determine the type of protons within the structure of the isolated lignin. Signal assignment

for 1H NMR were adopted from the early work of Tejado et al. (Tejado et al.). The acetylation of the lignin helped to reveal much defined proton signals in particular in the regions 9.0-6.0 and 3.0-0.9 ppm (Figure 3.3). Although the 1H NMR spectrum of the non-acetylated lignin indicates that the feedstock naturally contains aromatic and aliphatic acetyl groups (Figure 3.3b), the upgraded signals in the acetyl region (2.5-1.9 ppm) of the acetylated lignin spectrum (Figure 3.3a) allowed the determination of the relative distribution between original OH groups (Glasser and Jain). The ratio of normalized areas between the hydrogens in aromatic acetates and the hydrogens in aliphatic acetates, 5:15, confirms the predominance of aliphatic –OH groups (α-OH, ϒ-OH and β-OH) and thus the existence of long side-aliphatic oxygenated chains.

Finally, the use of thermogravimetric analysis helped us to reveal the main features of the thermal degradation behavior for the raw and coated materials. Dynamic measurements indicated that the thermal stability of LI20 remained the same than that of Pine starting to degrade at 180 °C, whereas the initial degradation temperature of LI40 was decreased to 145 °C. This was attributed to the larger addition of lignin that degrades at 126 °C (Figure 3.4). The maximum temperature of degradation also varied shifting towards higher temperatures from 399°C for the pine to 405 °C for both coated materials. This result was found in accordance with the well-known slow decomposition of lignins over a broad temperature range (M. Carrier, A. Loppinet-Serani, et al.; Jakab, Faix and Till) between 126-850 °C for this study (Figure 3.2).

The "synergetic effect", ΔM, that occurred during the pyrolysis of coated materials have been illustrated by plotting the difference in weight loss (ΔW) between the coated

material and each material in the blend, which have been weighted by their weight fraction, $x_i$ ($\Delta W = Wblend – (\Sigma x_i W_i)$). This analysis of synergetic effect, combining ΔM and DTG curves, that has been previously implemented by Cai et al. (Cai et al.) and lately by Ko et al. (Ko, Rawal and Sahajwalla), associates the negative values and dα/dt values close to zero with the formation of char, whereas positive values and non-null values of dα/dt could correspond to interactions between volatiles. Based on this, it clearly appears that coated materials are degraded in different ways (Figure 3.5). The pyrolysis of the coated material LI20 led to the formation of char occurring at two distinct stages, between 95-210 °C and 550-599 °C, , whereas most of the char was formed in one char-forming stage between 95 and 162 °C for LI40. The generation of the `primary char´ could be attributed to (i) the dehydration of biomass and (ii) the release of volatile matter that remains retained at the interface between the biomass particle and lignin layer. Whereas the formation of the `secondary char´ may be due to (iii) reactions between highly reactive volatiles from both materials and/or (iv) the cross-linking nature of lignin.

A second synergetic event as illustrated by the positive values of ΔM appeared in both cases. Its temperature range matched perfectly that of the maximum rate of devolatilization (for dα/dt values above 0.4 min-1), which indicates an enhanced release of volatiles when the blend is pyrolyzed. Differences in weight losses between coated materials could be then attributed to the presence and the thickness of the coating layer that varies according the preparation. Indeed, the scanning electron microscopy (SEM) images of the longitudinal and transversal sections of coated particles (Figure 3.6) confirm the deposit of extracted lignin particles onto the surface of pine biomass and into its pores; thus providing

an even coating over the entire surface. Also, the homogeneous and increasing brownish coloring of the coated material confirmed the presence of this layer, whose thickness depends on the amount of lignin added. The thicker layer found for LI40 could have then prevented the release of the volatile matter in a larger extent as suggested by the higher negative values of ΔW (Figure 3.5b).

## 3.2 Fast pyrolysis of raw and coated feedstocks

### 3.2.1 Yields of pyrolysis product

The preparation of coated feedstock allowed the fast pyrolysis of technical lignin lowering the bio-oil yields from 52.3 wt% for pine to 46.2 wt% and 46.6 wt% for LI20 and LI40, respectively (Table 3.2). This result represents a significant improvement regarding the low yields and technical issues obtained in the case of lignin (Nowakowski et al.). It is not surprising that char yield increased as the lignin content increased. Indeed, the reactor temperature of 540 °C could have not been high enough to fully pyrolyze the lignin, which is also considered as a precursor of char (Hosoya, Kawamoto and Saka "Cellulose-Hemicellulose and Cellulose-Lignin Interactions in Wood Pyrolysis at Gasification Temperature").

The yield of organics decreased from 37.84 wt% to 31.11-32.25 wt% when the isolated lignin was added, while the pyrolytic water yield increased from 4.96 wt% to 10.97-11.27 wt% (Table 3.2); thus indicating that the presence of the isolated lignin affects the chemistry of pyrolysis by promoting the dehydration reactions. Although the origin of the reactive water is often attributed to the presence of intramolecular dehydration reactions

occurring during the decomposition of hemicelluloses (Patwardhan, Brown and Shanks), it has also been suggested that the covalent bonding existing between virgin lignin and hemicelluloses could significantly affect the production of pyrolytic water and organics (M. Carrier, J. E. Joubert, et al.). In the present study, the substantial production of reactive water was clearly attributed to the presence of the isolated lignin.

Common views on natural polymer pyrolysis indicate that the efficient depolymerization with the production of organics is conditioned by the presence of oxygen and inter- and intramolecular hydrogen transfer reactions (Kotake, Kawamoto and Saka). In this case, the low oxygen content of coating material was beneficial to the formation of liquids, whereas the nature of the extracted lignin with the presence of aliphatic and oxygenated chains and non-transferable hydrogens prevented the efficient cleavage of alkyl-aryl ether linkages leading to the substantial formation of char (Hosoya, Kawamoto and Saka "Secondary Reactions of Lignin-Derived Primary Tar Components").

### 3.2.2 Bio-oil characterization

To better understand the chemical effect of this technical lignin on biomass pyrolysis mechanisms, the determination of the overall and partial relative product distribution and absolute concentration of key compounds were conducted.

The relative distribution of overall functional groups present in the pyrolysis bio-oils was determined via 13C NMR (Figure 3.7). Significant differences between the compositions of bio-oils were found. If the integration results for Pine were found in line with previous works (Ben and Ragauskas "Comparison for the Compositions of Fast and Slow Pyrolysis

Oils by Nmr Characterization"), the addition of the isolated lignin led to an increased formation of aliphatics, by 29 % for LI40 and 36 % for LI20 in comparison to the initial percentage obtained for the pine (Figure 3.7). Opposite trends were observed with respect to total aromatics (Aromatic C-O, aromatic C-C and aromatic C-H) with the decrease of total aromatics between 18% for LI40 and 23% for LI20. The slight decrease in the relative percentage of oxygenated aromatics may be explained by the addition of lignin of lower oxygen content (Table 3.1).

The preparation of coated biomass with increasing lignin did not increase the relative abundance of total aromatics as expected, but instead increased that of aliphatics, confirming that the hydrogens limited to the aliphatic and oxygenated side chains and aromatic rings of the technical lignin were not transferred to prevent the formation of char (Hosoya, Kawamoto and Saka "Pyrolysis Gasification Reactivities of Primary Tar and Char Fractions from Cellulose and Lignin as Studied with a Closed Ampoule Reactor"), but instead could activate the release of the same aliphatic and oxygenated chains (Figures 3.2 and 3.3).

Despite detecting only a portion of the bio-oil composition (Mohan, Pittman and Steele), the relevant chromatographic peaks were combined by chemical families to visualize changes between the relative functional group distribution with increasing amount of technical lignins. The organics were classified into thirteen groups including alcohols, ketones, aldehydes, acids, furans, compounds with a ring of 5 carbons (5-Cs), esters, anhydrosugars, phenolics, guaiacols, benzaldehydes and others (Figure 3.8a-c). In this case, the GC-MS technique allowed the analysis of both liquids. The first fraction recovered from the first condensation stage via indirect cooling contact at 4 degrees contains many light

oxygenated compounds (Figure 3.8a) and a large amount of water content between 33-38 wt%. On the other hand, the tarry phase with a lower water content in the range of 4.8-6.3 wt% collected from the second condensation stage via an electrostaticprecipitator contains a large aromatic portion (Figure 3.7) that is partially composed of phenolics and guaiacols (Figure 3.8b). Although GC/MS only detects the volatiles and monomeric phenolics and not dimers, trimers, tetramers, it was observed that the addition of lignin affected the chemical composition of both aqueous and organic fractions (Figure 3.8a-c).

For example, the acids content in aqueous phase increased gradually and significantly with the addition of technical lignin (Figure 3.8c), trend that was corroborated by the significant increase of the aliphatic fraction depicted by the 13C NMR analysis (Figure 3.7) and the quantification of acetic acid concentration (Table 3.3). This result was attributed to the degradation of the saturated aliphatic and oxygenated side-chains into light compounds (e.g., acetic acid and water).

However, the changes with respect to other organics, in particular for phenolics and guaiacols that could not be depicted by the 13C NMR analysis, did not follow a gradual trend in accordance with the increasing addition of lignin (Figure 3.8). In the case of LI20, an expected increase in phenolics that corresponded to a significant decrease in guaiacols was observed (Figure 3.8b). While a larger amount in lignin reversed the trends up to displaying a similar functional groups distribution than that of the uncoated material for the tarry phase (Figure 3.8b).

The significant increase in the phenolics accompanied with the decrease in guaiacols is not surprising, as the formation of monomeric phenolic compounds via free radical

reactions has been often reported during the pyrolysis of isolated and native lignins (Hosoya, Kawamoto and Saka "Secondary Reactions of Lignin-Derived Primary Tar Components"; Hosoya, Kawamoto and Saka "Pyrolysis Gasification Reactivities of Primary Tar and Char Fractions from Cellulose and Lignin as Studied with a Closed Ampoule Reactor"). In addition, the careful revision of the products separated by the GC-MS and of their MS spectrum led us to point out the presence of a phthalate ester with base peaks of m/z 207, 149 and 104 (Yin et al.); thus indicating that the phenols could have been further degraded in phthalate esters through the reactions of benzene radical, carbon dioxide and other alkyl radicals (Zeng et al.; Shen et al.).

The drastic change in chemical composition of aromatics between LI20 and LI40 can also be attributed to the thicker layer of lignin, which prevented/slowed down the release of volatiles as mentioned in the section 3.1. The same layer could have prevented the guaiacols to be further degraded into phenols and catechols and subsequently into phthalates, reaction that was reported to occur in a gas phase (Shen et al.).

The determination of absolute concentration of key organics involved into the biomass pyrolysis was also carried out. The selection of the key compounds was based on previous studies that described in detail the pyrolysis mechanisms of major polymers that composed the lignocellulosic biomass (i.e., hemicelluloses, cellulose and lignin) (Patwardhan, Brown and Shanks; Patwardhan, Dalluge, et al.; Azeez et al.). As a result levoglucosan (LG), acetol (AC) and glycoaldehyde (GA) were selected to follow the cellulose pyrolysis, while phenol, phenol, 4-methyl and phenol, 2-methoxy-4-methyl were chosen as lignin-derived products. The concentrations expressed on a weight basis of dry

feed of cellulose-derived products, LG, AC and GA, remained the same or decreased with the addition of lignin (Table 3.3). When a gradual decrease in the carbohydrate-derived products could have been expected considering the lower proportion in carbohydrates to be pyrolyzed, the pyrolysis of LI20 led to higher levels in furfural and acetol in comparison to LI40.

The trends observed for the lignin-derived products (i.e., phenol, phenol, 4-methyl and Phenol, 2-methoxy-4-methyl) levels, with an increasing production of phenols and a decreasing formation of guaiacols for LI20 were found in accordance with the functional group distribution (Figure 3.8). These results indicate that the decomposition of ether bond in lignin was more efficient in the case of small addition of technical lignin, while the addition of a larger amount have led to the formation of more stable guaiacols. If the guaiacols and phenolics are often reported as main decomposition products of aryl-ether bonds, guaiacols are further converted into catechols with increasing temperature (Ben and Ragauskas "Nmr Characterization of Pyrolysis Oils from Kraft Lignin"); thus confirming the higher thermal stability of some guaiacols.

The levels of acetic acid increased significantly with the increase of lignin content (Table 3.3), suggesting that the additional acid formed originates from acetoxy groups present in the isolated lignin, thus supporting the speculative free-radical chain reaction proposed by Shen et al. (Shen et al.). It is noteworthy that the acetic acid is a catalyst for oligomerizing phenolic compounds that could be formed via recombination/re-oligomerization of the primary pyrolysis products of lignin during the condensation process (Patwardhan, Brown and Shanks). It is then suspected that the sufficient levels of acetic acid

produced during the fast pyrolysis of LI40 could have promoted the oligomerization of phenolic compounds, thus lowering their content (Figure 3.8c). This observation supports the reoligomerization model through radical mechanisms (Bai et al.) for the formation of phenolic oligomer instead of the thermal-mechanical ejection (Teixeira et al.).

## 4. Conclusions

This work has demonstrated the possibility of fast pyrolyzing a problematic feedstock, a purified lignin, with Pinus Radiata sawdust. To do this, a new coating preparation method was developed. This technique consists in a wet impregnation technique, mixing the extracted lignin powder already dissolved in acetone with Pinus radiata sawdust. Conventional fast pyrolysis of the coated material was carried out at 540 °C using a fluidized bed reactor. Although a slight decrease in total liquid and organic yields were observed when both coated materials, LI20 and LI40, were pyrolyzed, no technical issues such as bed agglomeration, feeding plugs or solid entrainment occurred. As the lignin addition increased, char, pyrolytic water yields and acids content increased. These changes were attributed to the presence of aliphatic and oxygenated side-chains within the isolated lignin's structure.

The thermal evaluation of coated materials and the in-depth characterization of both raw materials and fast pyrolysis bio-oils helped us to point out drastic mechanistic changes during the fast pyrolysis in the specific case of LI20, for which an intermediate amount of lignin was added. These changes were associated with the presence of the fine and impermeable layer preventing the release of pyrolysis volatiles. In the case of LI40, it was

speculated that the substantial formation of acetic acid could have catalyzed re-oligomerization reactions lowering the content of monomeric phenolics.

## 5. Acknowledgements

The financial support for this project came from the Project Basal PFB-27 and the Program PMI InEs UCO-1302 of the Chilean Ministry of Education. Ms. Karen Lyssette Bustamante Tassara (CESMI) is acknowledged for performing the NMR analyses.

## REFERENCES


Azeez, A. M., et al. "Fast Pyrolysis of African and European Lignocellulosic Biomasses Using Py-Gc/Ms and Fluidized Bed Reactor." *Energy & Fuels* 24 (2010): 2078-85. Print.

Bai, X. L., et al. "Formation of Phenolic Oligomers During Fast Pyrolysis of Lignin." *Fuel* 128 (2014): 170-79. Print.

Beis, S. H., et al. "Fast Pyrolysis of Lignins." *Bioresources* 5.3 (2010): 1408-24. Print.

Ben, H. X., and A. J. Ragauskas. "Comparison for the Compositions of Fast and Slow Pyrolysis Oils by Nmr Characterization." *Bioresource Technology* 147 (2013): 577-84. Print.

---. "Nmr Characterization of Pyrolysis Oils from Kraft Lignin." *Energy & Fuels* 25.5 (2011): 2322-32. Print.

Berg, A., C. Fuentealba, and J. P. Salazar. "Separation of Lignocellulosic Components in Acetic Acid Media and Evaluation of Applications." *J-for-Journal of Science & Technology for Forest Products and Processes* 3.6 (2013): 27-32. Print.

Cai, J. Q., et al. "Thermogravimetric Analysis and Kinetics of Coal/Plastic Blends During Co-Pyrolysis in Nitrogen Atmosphere." *Fuel Processing Technology* 89.1 (2008): 21-27. Print.

Carrier, M., et al. "Impact of the Lignocellulosic Material on Fast Pyrolysis Yields and Product Quality." *Bioresource Technology* 150 (2013): 129-38. Print.

Carrier, M., et al. "Thermogravimetric Analysis as a New Method to Determine the Lignocellulosic Composition of Biomass." *Biomass & Bioenergy* 35.1 (2011): 298-307. Print.

Carrier, Marion, et al. "Depolymerization of Acetosolv Lignin through in-Situ Catalytic Fast Pyrolysis." *de la Facultad de Ciencias Químicas* (2014): 61. Print.

Case, P. A., et al. "Pyrolysis of Pre-Treated Tannins Obtained from Radiata Pine Bark." *Journal of Analytical and Applied Pyrolysis* 107 (2014): 250-55. Print.

De Wild, P. J., W. J. J. Huijgen, and R. J. A. Gosselink. "Lignin Pyrolysis for Profitable Lignocellulosic Biorefineries." *Biofuels Bioproducts & Biorefining-Biofpr* 8.5 (2014): 645-57. Print.

de Wild, P. J., W. J. J. Huijgen, and H. J. Heeres. "Pyrolysis of Wheat Straw-Derived Organosolv Lignin." *Journal of Analytical and Applied Pyrolysis* 93 (2012): 95-103. Print.

de Wild, Paul, Hans Reith, and Erik Heeres. "Biomass Pyrolysis for Chemicals." *Biofuels* 2.2 (2011): 185-208. Print.

Dondi, D., et al. "The Role of Inorganic Sulfur Compounds in the Pyrolysis of Kraft Lignin." *Journal of Analytical and Applied Pyrolysis* 107 (2014): 53-58. Print.

Feng, S. H., et al. "Valorization of Bark for Chemicals and Materials: A Review." *Renewable & Sustainable Energy Reviews* 26 (2013): 560-78. Print.

Fernandez-Costas, C., et al. "Structural Characterization of Kraft Lignins from Different Spent Cooking Liquors by 1d and 2d Nuclear Magnetic Resonance Spectroscopy." *Biomass & Bioenergy* 63 (2014): 156-66. Print.

Glasser, Wolfgang G, and Rajesh K Jain. "Lignin Derivatives. I. Alkanoates." *Holzforschung-International Journal of the Biology, Chemistry, Physics and Technology of Wood* 47.3 (1993): 225-33. Print.

Gosselink, R. J. A., et al. "Co-Ordination Network for Lignin - Standardisation, Production and Applications Adapted to Market Requirements (Eurolignin)." *Industrial Crops and Products* 20.2 (2004): 121-29. Print.

Hosoya, T., H. Kawamoto, and S. Saka. "Cellulose-Hemicellulose and Cellulose-Lignin Interactions in Wood Pyrolysis at Gasification Temperature." *Journal of Analytical and Applied Pyrolysis* 80.1 (2007): 118-25. Print.

---. "Pyrolysis Gasification Reactivities of Primary Tar and Char Fractions from Cellulose and Lignin as Studied with a Closed Ampoule Reactor." *Journal of Analytical and Applied Pyrolysis* 83.1 (2008): 71-77. Print.

---. "Secondary Reactions of Lignin-Derived Primary Tar Components." *Journal of Analytical and Applied Pyrolysis* 83.1 (2008): 78-87. Print.

Jakab, E., O. Faix, and F. Till. "Thermal Decomposition of Milled Wood Lignins Studied by Thermogravimetry Mass Spectrometry." *Journal of Analytical and Applied Pyrolysis* 40-1 (1997): 171-86. Print.

Jones, B. W., et al. "Enhancement in Enzymatic Hydrolysis by Mechanical Refining for Pretreated Hardwood Lignocellulosics." *Bioresource Technology* 147 (2013): 353-60. Print.

Jung, S. H., et al. "Pyrolysis of a Fraction of Waste Polypropylene and Polyethylene for the Recovery of Btx Aromatics Using a Fluidized Bed Reactor." *Fuel Processing Technology* 91.3 (2010): 277-84. Print.

Ko, Kwang-Hyun, Aditya Rawal, and Veena Sahajwalla. "Analysis of Thermal Degradation Kinetics and Carbon Structure Changes of Co-Pyrolysis between Macadamia Nut Shell and Pet Using Thermogravimetric Analysis and 13 C Solid State Nuclear Magnetic Resonance." *Energy Conversion and Management* 86 (2014): 154-64. Print.

Kotake, T., H. Kawamoto, and S. Saka. "Mechanisms for the Formation of Monomers and Oligomers During the Pyrolysis of a Softwood Lignin." *Journal of Analytical and Applied Pyrolysis* 105 (2014): 309-16. Print.

Kubo, S., and J. F. Kadla. "Hydrogen Bonding in Lignin: A Fourier Transform Infrared Model Compound Study." *Biomacromolecules* 6.5 (2005): 2815-21. Print.

Li, D. B., C. Briens, and F. Berruti. "Improved Lignin Pyrolysis for Phenolics Production in a Bubbling Bed Reactor - Effect of Bed Materials." *Bioresource Technology* 189 (2015): 7-14. Print.

Lin, Y. Y., et al. "Deoxygenation of Bio-Oil During Pyrolysis of Biomass in the Presence of Cao in a Fluidized-Bed Reactor." *Energy & Fuels* 24 (2010): 5686-95. Print.

Meng, J. J., et al. "The Effect of Torrefaction on the Chemistry of Fast-Pyrolysis Bio-Oil." *Bioresource Technology* 111 (2012): 439-46. Print.

Mohan, D., C. U. Pittman, and P. H. Steele. "Pyrolysis of Wood/Biomass for Bio-Oil: A Critical Review." *Energy & Fuels* 20.3 (2006): 848-89. Print.

Nowakowski, D. J., et al. "Lignin Fast Pyrolysis: Results from an International Collaboration." *Journal of Analytical and Applied Pyrolysis* 88.1 (2010): 53-72. Print.

Oasmaa, A., et al. "Fast Pyrolysis Bio-Oils from Wood and Agricultural Residues." *Energy & Fuels* 24 (2010): 1380-88. Print.

Park, H. J., Y. K. Park, and J. S. Kim. "Influence of Reaction Conditions and the Char Separation System on the Production of Bio-Oil from Radiata Pine Sawdust by Fast Pyrolysis." *Fuel Processing Technology* 89.8 (2008): 797-802. Print.

Patwardhan, P. R., R. C. Brown, and B. H. Shanks. "Product Distribution from the Fast Pyrolysis of Hemicellulose." *Chemsuschem* 4.5 (2011): 636-43. Print.

Patwardhan, P. R., et al. "Distinguishing Primary and Secondary Reactions of Cellulose Pyrolysis." *Bioresource Technology* 102.8 (2011): 5265-69. Print.

Patwardhan, Pushkaraj Ramchandra. "Understanding the Product Distribution from Biomass Fast Pyrolysis." (2010). Print.

Shen, D. K., et al. "The Pyrolytic Degradation of Wood-Derived Lignin from Pulping Process." *Bioresource Technology* 101.15 (2010): 6136-46. Print.

Sluiter, A, et al. "Determination of Extractives in Biomass." *Laboratory Analytical Procedure (LAP)* 1617 (2005). Print.

Teixeira, A. R., et al. "Aerosol Generation by Reactive Boiling Ejection of Molten Cellulose." *Energy & Environmental Science* 4.10 (2011): 4306-21. Print.

Tejado, A., et al. "Physico-Chemical Characterization of Lignins from Different Sources for Use in Phenol-Formaldehyde Resin Synthesis." *Bioresource Technology* 98.8 (2007): 1655-63. Print.

Wilkomirsky, I, E Moreno, and A Berg. "Bio-Oil Production from Biomass by Flash Pyrolysis in a Three-Stage Fluidized Bed Reactors System." *Journal of Materials Science and Chemical Engineering* 2014 (2014). Print.

Wyman, Charles E. *Aqueous Pretreatment of Plant Biomass for Biological and Chemical Conversion to Fuels and Chemicals*. John Wiley & Sons, 2013. Print.

Xiu, S. N., and A. Shahbazi. "Bio-Oil Production and Upgrading Research: A Review." *Renewable & Sustainable Energy Reviews* 16.7 (2012): 4406-14. Print.

Yin, P., et al. "Mass Spectral Fragmentation Pathways of Phthalate Esters by Gas Chromatography-Tandem Mass Spectrometry." *Analytical Letters* 47.9 (2014): 1579-88. Print.

Zakzeski, J., et al. "The Catalytic Valorization of Lignin for the Production of Renewable Chemicals." *Chemical Reviews* 110.6 (2010): 3552-99. Print.

Zeng, F. X., et al. "Separation of Phthalate Esters from Bio-Oil Derived from Rice Husk by a Basification-Acidification Process and Column Chromatography." *Bioresource Technology* 102.2 (2011): 1982-87. Print.

Zhou, C. F., et al. "Prediction of Mixed Hardwood Lignin and Carbohydrate Content Using Atr-Ftir and Ft-Nir." *Carbohydrate Polymers* 121 (2015): 336-41. Print.

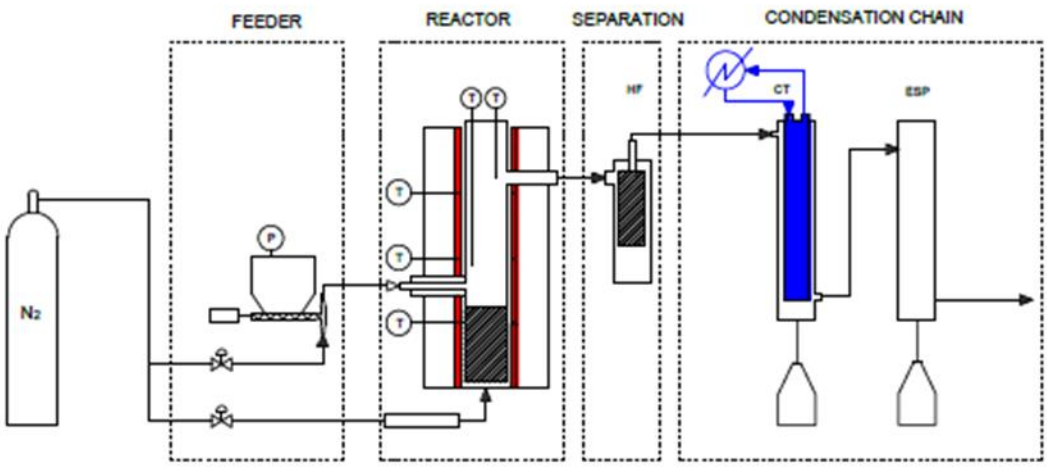


**Figure 3.1** Fast pyrolysis set-up showing the four sections.

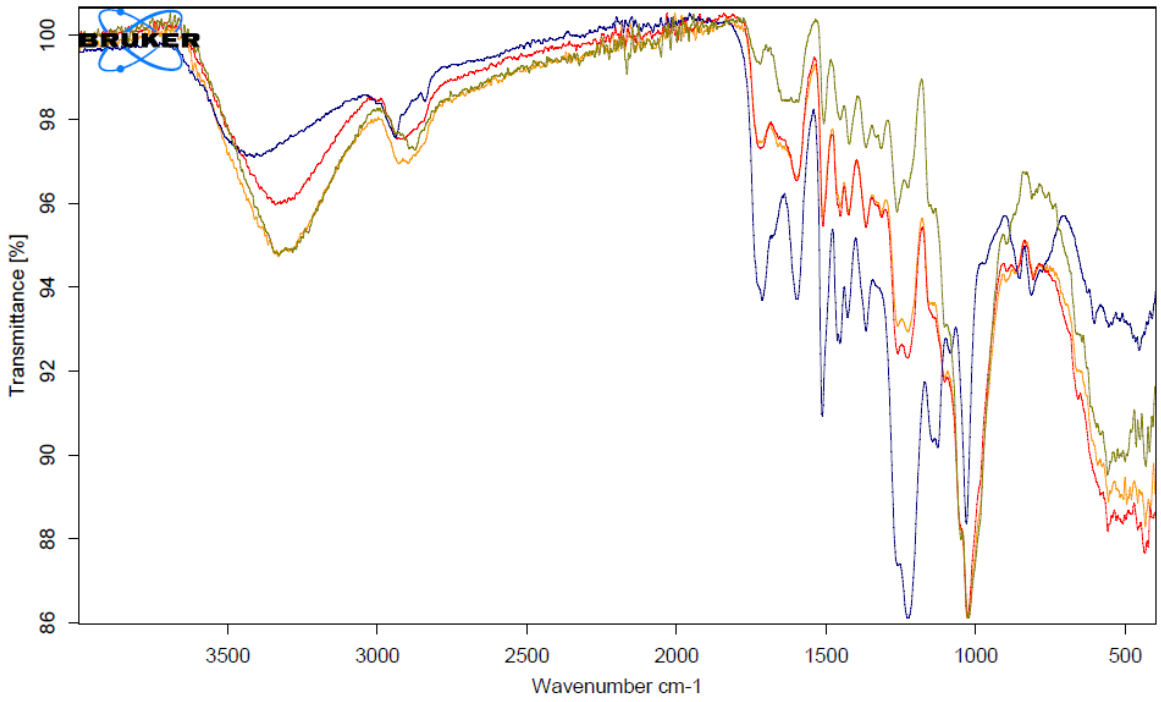


**Figure 3.2** ATR-FTIR spectra of raw and coated materials. Gold-Radiata Pine, Blue-Acetosolv lignin, Red- $LI_{20}$, Yellow-$LI_{40}$.

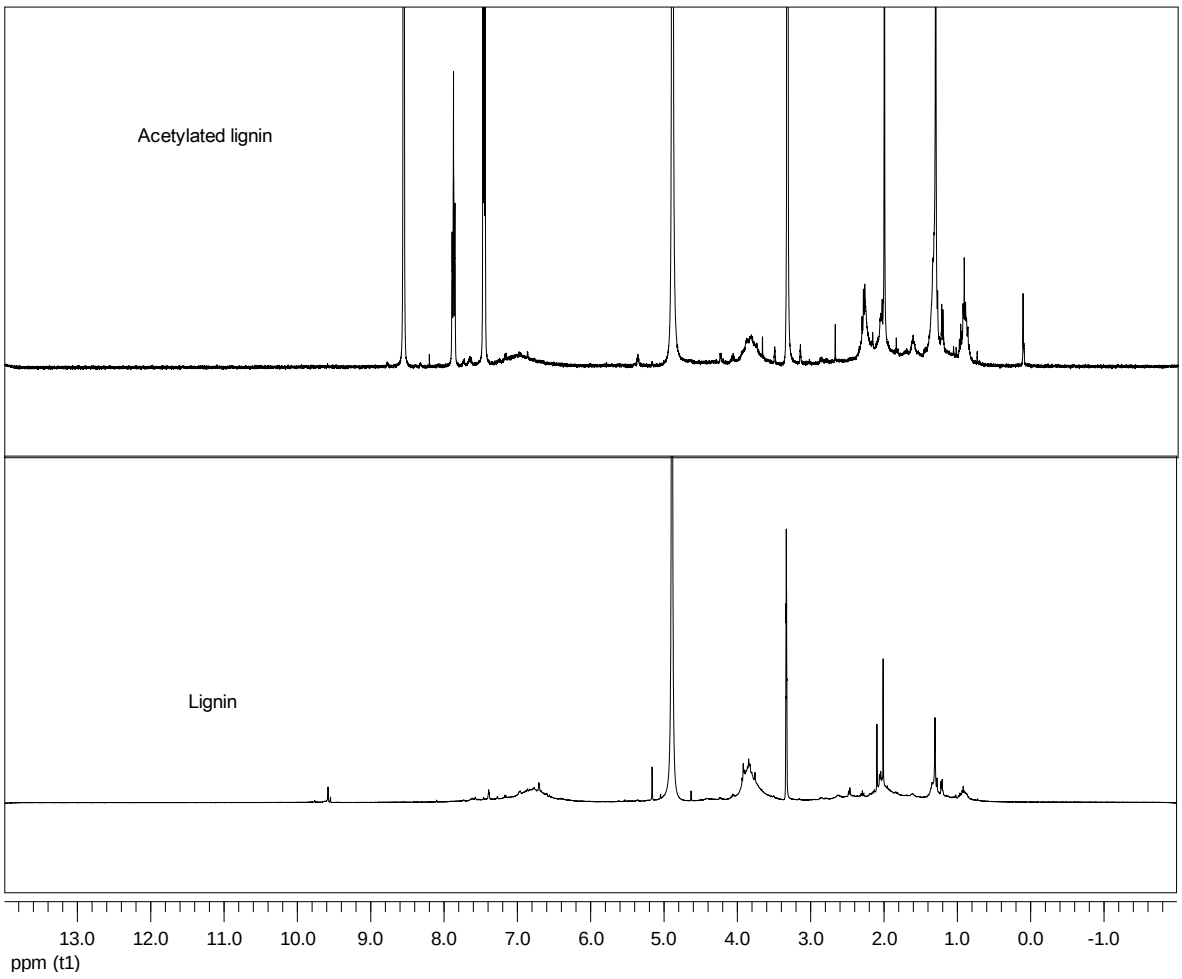


**Figure 3.3** $^{1}$H NMR spectra of a) the acetylated and b) non-acetylated lignins with the following signal assignments: 10.0-9.7 ppm for H in benzaldehyde units, 8.0-6.0 ppm for aromatic H in sinapyl (S) and G units, 4.2-3.1 ppm for methoxyl H, 2.5-2.2 ppm for H in aromatic acetates, 2.2-1.9 for H in aliphatic acetates and 1.5-0.8 ppm for aliphatic H.

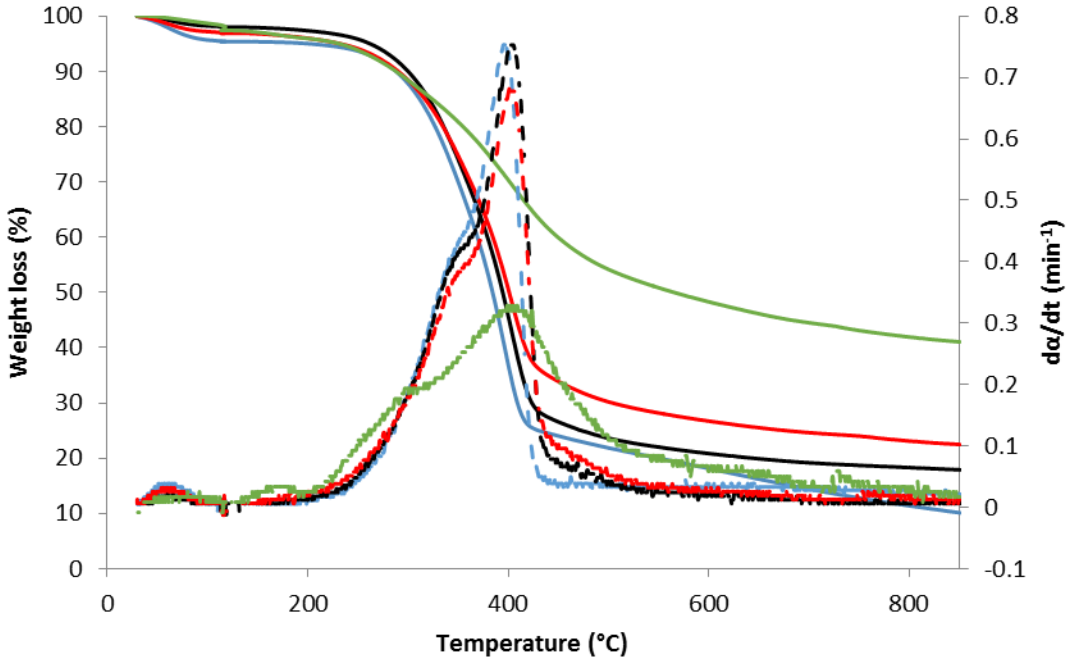


**Figure 3.4** Thermogravimetric and derivative curves for the raw materials. TGA curves are solid lines and DTG curves are dashed. Blue- Radiata Pine, Green-Acetosolv lignin, Black-$LI_{20}$, Red- $LI_{40}$.

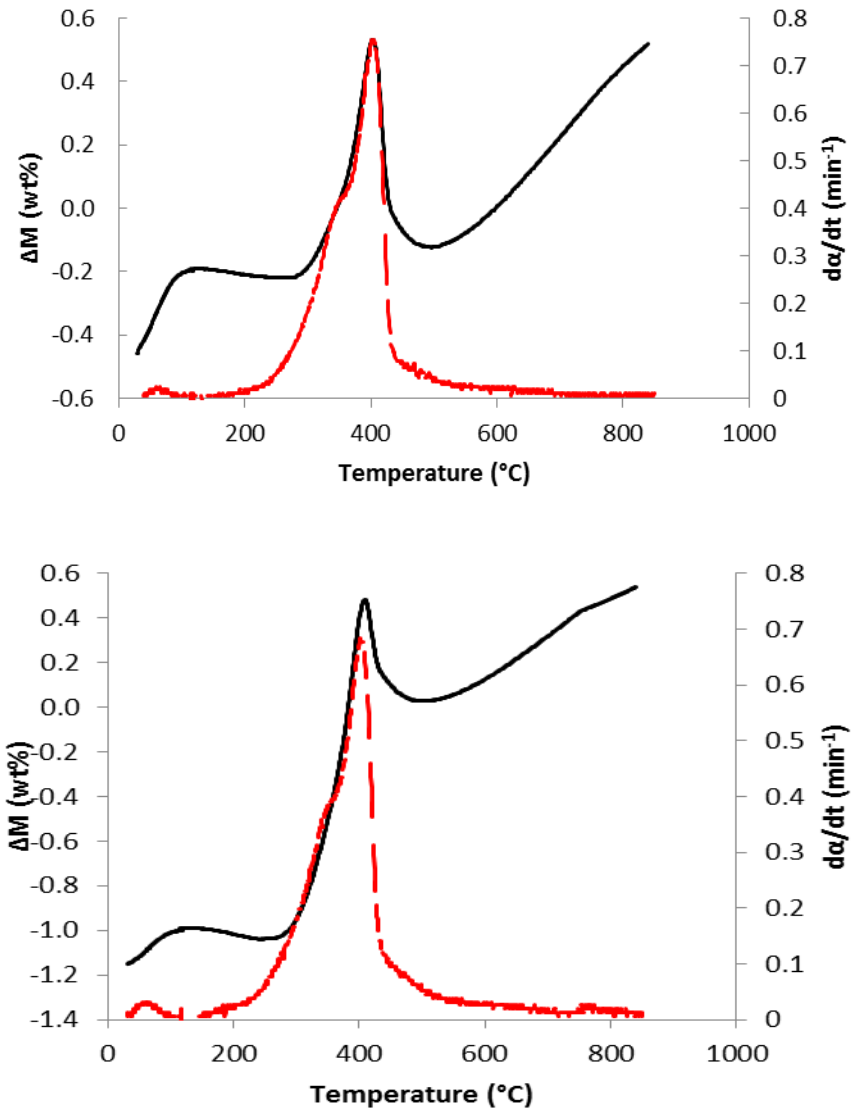


**Figure 3.5** Synergetic effect (ΔM)-Black and derivated thermogravimetric curves (dα/dt)-Red for $LI_{20}$- top and $LI_{40}$- bottom.

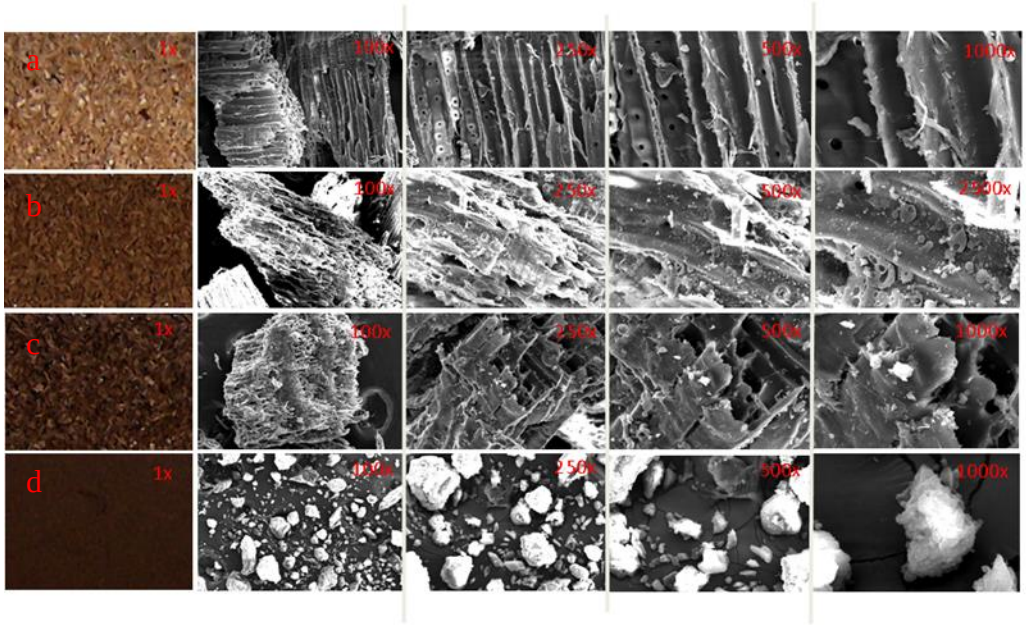


**Figure 3.6** SEM photos of a) Pine, b) LI20, c) LI40 and d) Acid-extracted lignin powder.

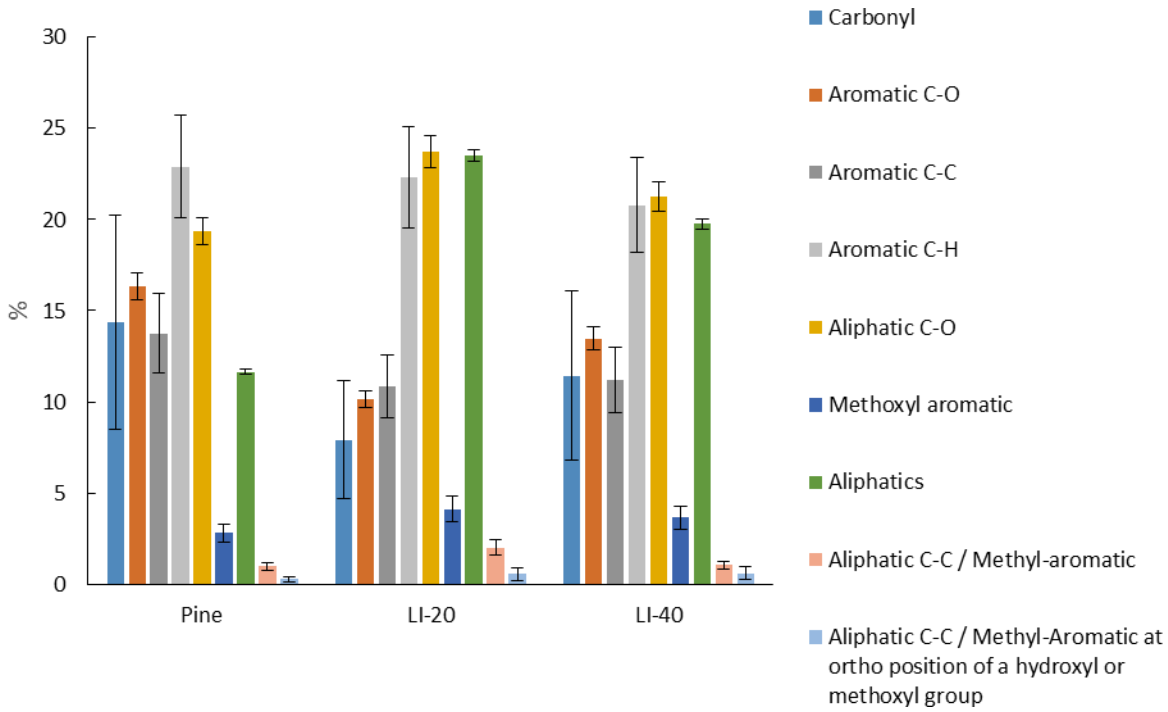


**Figure 3.7** Relative percentages of functional groups determined by $^{13}C$ NMR for the BOP fraction.

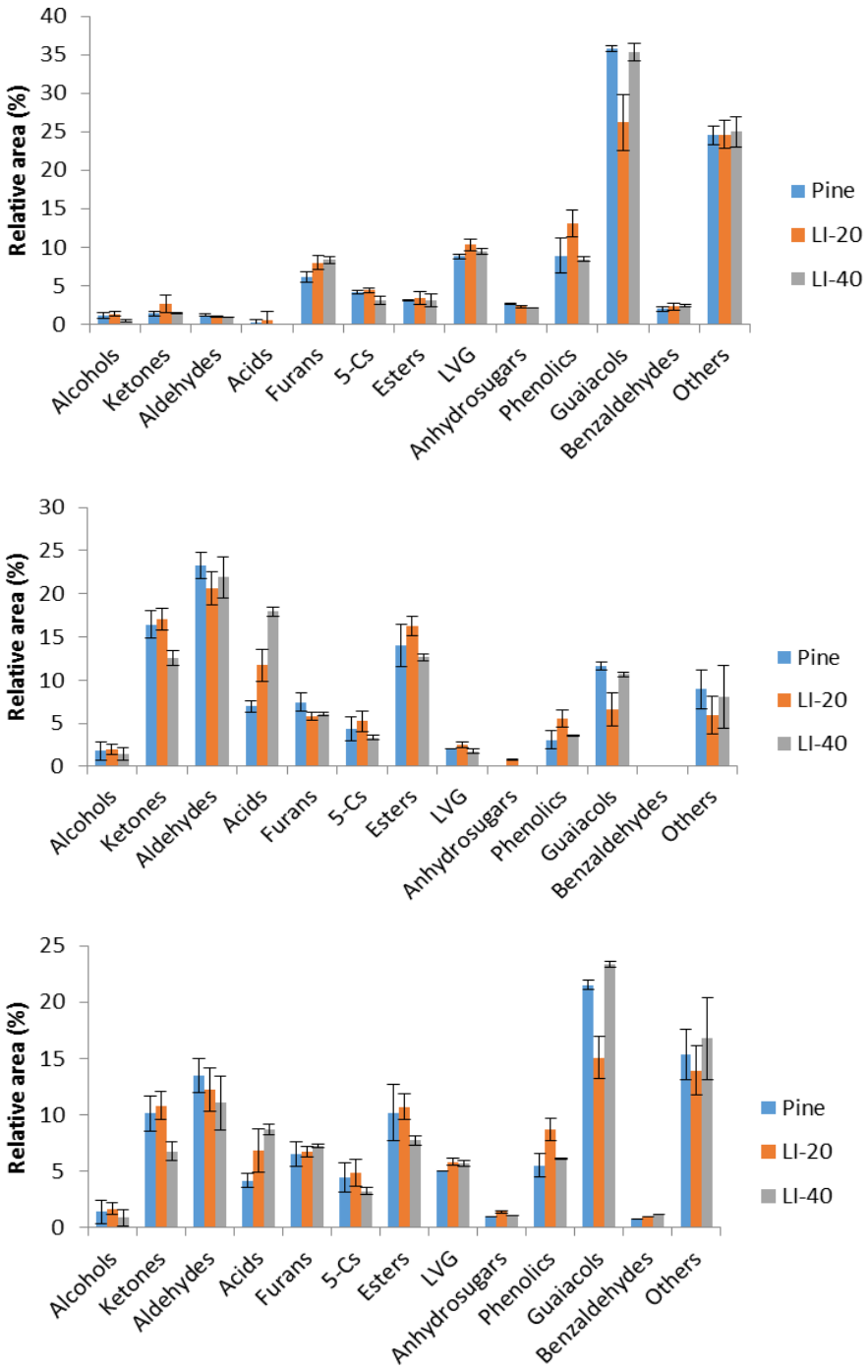


**Figure 3.8** Relative percentage of product distribution for the BOC fraction (top), the BOP fraction (middle), and combined fractions (bottom).

**Table 3.1** Compositional and physico-chemical properties of feedstock.

| | ***Pinus Radiata*** | **$LI_{20}$** | **$LI_{40}$** | **Acetosolv Lignin** |
|---|---|---|---|---|
| Moisture content | 5.24 ±1.37 | 3.97 ± 1.08 | 5.61±1.42 | 4.74 ± 0.72 |
| **Compositional analysis (wt%)** | | | | |
| **Carbohydrates** | 47.54 ±1.25 | 41.40 ± 0.21 | 36.32 ± 0.58 | 3.77 ± 0.26 |
| Glucan | 43.34 ± 1.09 | 37.87±0.16 | 33.46 ± 0.53 | 4.00 ± 0.23 |
| Xylan | 3.48 ± 0.08 | 3.04 ± 0.09 | 2.26 ± 0.07 | 0.00 ± 0.00 |
| Galactose | 0.72 ± 0.08 | 0.48 ± 0.07 | 0.24 ± 0.01 | 0.00 ± 0.04 |
| **Lignin** | 32.78 ± 0.74 | 38.30 ± 0.47 | 46.83 ± 1.40 | 97.19 ± 0.29 |
| Acid Insoluble Residue (AIR) | 32.23 ± 0.72 | 37.67± 0.45 | 45.87 ± 1.30 | 95.11 ± 0.17 |
| Acid Soluble Lignin (ASL) | 0.55 ± 0.02 | 0.63 ± 0.02 | 0.96 ± 0.10 | 2.08 ± 0.12 |
| **Extractives** | | | | |
| Hexane | 0.95 ± 0.03 | | | |
| Water | 2.91 ± 0.08 | | | |
| Ethanol | 1.95 ± 0.11 | | | |
| **Ash** | 0.89 | 0.80 | 1.15 | 0.56 |
| **Mass balance** | 92.26 | 84.47 | 89.91 | 106.26 |
| **Ultimate analysis (db, wt%)** | | | | |
| C | 48.18 ± 0.92 | 48.55 ± 0.20 | 51.37 ± 0.41 | 65.98 ± 0.11 |
| H | 5.61 ± 0.10 | 5.76 ± 0.37 | 5.44 ± 0.34 | 5.52 ± 0.38 |
| N | 0.07 ± 0.02 | 0.07 ± 0.02 | 0.07 ± 0.03 | 0.11 ± 0.01 |
| O | 49.74 ± 0.84 | 46.64 ± 0.30 | 44.84 ± 0.48 | 30.22 ± 0.54 |
| **Proximate analysis (db, wt%)** | | | | |
| VM | 94.70 | 84.25 | 78.37 | 59.58 |
| FC | 4.38 | 14.93 | 20.48 | 39.87 |
| AC | 0.92 | 0.82 | 1.15 | 0.55 |

**Table 3.2** Yield (Y) in db, wt% from fast pyrolysis experiments.

| | **Yoil** (db, wt%) | **Ychar** | **Ygas*** | **Yorganics** | **Ypyrolytic water** | **$Y_{BOC}$** (wt%) | **$Y_{BOP}$** | **Ratio BOP:BOC** (-) |
|---|---|---|---|---|---|---|---|---|
| **Pine** | 52.32 ± 3.96 | 9.68 ± 0.28 | 38.00 ± 4.15 | 37.84 ± 3.72 | 4.96 ± 0.51 | 35.0 ± 3.7 | 17.3 ± 0.2 | 0.50 ± 0.05 |
| **$LI_{20}$** | 46.24 ± 7.00 | 17.79 ± 4.79 | 35.97 ± 3.42 | 31.11 ± 1.41 | 11.27 ± 0.06 | 26.4 ± 3.3 | 19.8 ± 1.9 | 0.76 ± 0.17 |
| **$LI_{40}$** | 46.59 ± 6.09 | 18.87 ± 7.74 | 34.53 ± 1.65 | 32.25 ± 2.98 | 10.97 ± 3.49 | 23.7 ± 6.0 | 24.6 ± 7.3 | 1.03 ± 0.04 |

**Table 3.3** Product concentration in BOC and BOP fractions.

| | **Unit** | **Pine** | | **$LI_{20}$** | | **$LI_{40}$** | |
|---|---|---|---|---|---|---|---|
| | | **BOC** | **BOP** | **BOC** | **BOP** | **BOC** | **BOP** |
| Hydroxyacetaldehyde (Glycoaldehyde) | wt%, bio-oil | 9.3 | 2.21 | 5.86 | 2.21 | 5.8 | 2.18 |
| | wt%, dry bio-oil | 7.54* | | 5.19* | | 5.88* | |
| | wt% dry feed | 0.080 | | 0.065 | | 0.076 | |
| Acetic acid | wt%, bio-oil | 3.95 | 2.77 | 3.19 | 3.33 | **3.3** | 3.47 |
| | wt%,dry bio-oil | 4.16* | | 5.19* | | 5.88* | |
| | wt% dry feed | 0.044 | | 0.047 | | 0.053 | |
| 2-propanone, 1-hydroxy (Acetol) | wt%, bio-oil | 4.13 | 1.23 | 2.72 | 1.7 | 1.79 | 1.06 |
| | wt%,dry bio-oil | 3.26 | | 3.68 | | 2.78 | |
| | wt% dry feed | 0.034 | | 0.033 | | 0.025 | |
| Furfural | wt%, bio-oil | 0.12 | 0.29 | 0.11 | 0.46 | 0.09 | 0.34 |
| | wt%,dry bio-oil | 0.25 | | 0.39 | | 0.26 | |
| | wt% dry feed | 0.0027 | | 0.0034 | | 0.0024 | |
| Levoglucosan | wt%, bio-oil | 0.275 | 6.00 | 0.19 | 7.77 | 0.12 | 6.73 |
| | wt%,dry bio-oil | 4.09 | | 4.98 | | 3.53 | |
| | wt% dry feed | 0.043 | | 0.045 | | 0.032 | |
| Phenol | wt%, bio-oil | 0.03 | 0.16 | 0.07 | 0.38 | 0.03 | 0.26 |
| | wt%,dry bio-oil | 0.137 | | 0.300 | | 0.171 | |
| | wt% dry feed | 0.0015 | | 0.0027 | | 0.0015 | |
| Phenol, 4-methyl | wt%, bio-oil | 0 | 0.1 | 0 | 0.21 | 0 | 0.1 |
| | wt%,dry bio-oil | 0.019 | | 0.1000 | | 0.022 | |
| | wt% dry feed | 0.0002 | | 0.00090 | | 0.00020 | |
| Phenol, 2-methoxy-4-methyl | wt%, bio-oil | 0.07 | 0.6 | 0.02 | 0.55 | 0.06 | 0.89 |
| | wt%,dry bio-oil | 0.427 | | 0.359 | | 0.529 | |
| | wt% dry feed | 0.0045 | | 0.0034 | | 0.0048 | |

# CHAPTER 4

## Suggested Future Research

The aforementioned work focused on the effects of biomass properties on fast pyrolysis bio-oil. These three studies gave much insight into how the true nature of fast pyrolysis of lignocellulosic biomass can be understood. Based on this research several follow-up studies could be proposed to advance the knowledge further.

### Effect of Cellulose Degree of Polymerization at lower Chain Length

The experiments in Chapter 1 on DP of cellulose showed that levoglucosan content increased as the DP of the cellulose sample decreased. However, other research has shown that as DP increases, levoglucosan increases (Mettler et al.). There is however a gap in the DP of cellulose between the two studies. Mettler et al., used model compounds and started with DP of 1 and increased to DP 6, whereas the experiments performed here, the lowest DP measured was 500. There is a large gap between these values and it would be interesting and beneficial to reduce the DP to less than 100 or even lower if possible to see if there exists a maximum in levoglucosan production. Since levoglucosan is the primary decomposition product of cellulose, this would give an indication as to the ideal characteristics of cellulose for being broken down by fast pyrolysis.

**Acid and Base Pretreatment of Lignocellulosic Biomass for Fast Pyrolysis**

The addition of calcium formate via wet mixing with a reaction led to some unexpected results in Chapter 2. The dry mixing calcium formate did not have the desired effect on the bio-oil oxygen content. However, there clearly was a difference in the bio-oil produced from wet-mixing with a reaction. This could be due to the acid/base reactions that took place during the preparation process. It is well known that weak sulfuric acid can be used as a pretreatment for biochemical conversion of lignocellulosic biomass, but not much work has been done to investigate its use in thermochemical conversion (Nguyen et al.). Acids can be used to remove inorganics, such as minerals and ash, prior to fast pyrolysis, which can be beneficial (Patwardhan, Satrio, et al.). This proposed study could investigate various acids and bases at different concentrations, as well as different impregnation times, and amounts of acid or base. After washing or no washing and drying, the biomass should be subjected to fast pyrolysis and the products analyzed, along with the ultimate analysis and compositional analysis to determine how the biomass was changed during the pretreatment. This research could further explain the results in Chapter 2, while also opening up a possible pretreatment method to improve the bio-oil from fats pyrolysis.

**Large Scale Fast Pyrolysis**

The vast majority of the research in fast pyrolysis is at the lab-scale or smaller. This works well, but for more industrial uses, large scale trials need to be conducted. UDT in Concepcion, Chile was the site for much of the work in Chapter 3. The experiments were all performed at the lab-scale, however they have a 10kg/hr plant that would be ideal for testing

if the LI biomass can be fed and pyrolyzed at a much higher rate (Wilkomirsky, Moreno and Berg). If it can be fed, then analyzing the resulting bio-oil could provide a definite use for waste process lignin, while also allowing the results to be compared between large scale and lab scale for the same sample.

**Impregnation of Different Types of Lignin**

Organosolv lignin was used for the experiments in Chapter 3 as a representation of process lignin. This lignin was also used as a model to see how increasing the lignin content affected the bio-oil. Understandably, this lignin is not the ideal representative of native lignin and for a better representation, other lignin types could be investigated. Cellulolytic enzyme lignin is seen as one of the best and most native types of isolated lignin (GUERRA et al.). By adding CEL to the Pine biomass and pyrolyzing the samples, relationships could be formed based on the increase of lignin content in natural lignocellulosic biomass, and its effect on bio-oil. The experiments could be repeated also for milled wood lignin (MWL) and enzymatic mild acidolysis lignin (EMAL). Hypothetically the results shown would be solely from lignin and not from impurities from modified lignin.

## REFERENCES

GUERRA, ANDERSON, et al. "Toward a Better Understanding of the Lignin Isolation Process from Wood." Print.

Mettler, Matthew S., et al. "The Chain Length Effect in Pyrolysis: Bridging the Gap between Glucose and Cellulose." *Green Chemistry* 14.5 (2012): 1284. Print.

Nguyen, Quang A., et al. *Two-Stage Dilute-Acid Pretreatment of Softwoods*. Twenty-first Symposium on biotechnology for fuels and chemicals. 2000. Springer. Print.

Patwardhan, P. R., et al. "Influence of Inorganic Salts on the Primary Pyrolysis Products of Cellulose." *Bioresour Technol* 101.12 (2010): 4646-55. Print.

Wilkomirsky, I, E Moreno, and A Berg. "Bio-Oil Production from Biomass by Flash Pyrolysis in a Three-Stage Fluidized Bed Reactors System." *Journal of Materials Science and Chemical Engineering* 2014 (2014). Print.